

Theory for Anomalous NMR Response in $\text{Pb}_{1-x}\text{Tl}_x\text{Te}$ on Charge Kondo Effect

Kazumasa Miyake^{1*} and Hiroyasu Matsuura²

¹ *Center for Advanced High Magnetic Field Science, Osaka University, Toyonaka, Osaka 560-0043, Japan*

² *Department of Physics, University of Tokyo, Hongo, Bunkyo-ku, Tokyo 113-0033, Japan*

(Received June 4, 2018)

A theory for anomalous enhancement of NMR relaxation rate $1/T_1T$ of ^{125}Te toward zero temperature observed in $\text{Pb}_{1-x}\text{Tl}_x\text{Te}$ ($x=0.01$) is presented on the idea of the charge Kondo effect of valence skipping element Tl. It is found that such enhancement in $1/T_1T$ is caused through enhancement of the pair-hopping and inter-orbital interactions between 6s electrons localized on Tl site and conduction electrons doped in the hole band the semiconductor PbTe, which is the heart of the charge Kondo effect. It is also found that the Knight shift is not influenced in the temperature region where the relaxation rate is enhanced which is consistent with the experimental observation showing that the Korringa relation is apparently broken.

1. Introduction

In the past decade, valence skipping phenomenon and related superconductivity have caused revived attention since the charge Kondo effect and the superconductivity had been reported in $\text{Pb}_{1-x}\text{Tl}_x\text{Te}$ ($0.006 < x < 0.015$).¹⁾ Since the valence state of Pb is Pb^{2+} , the nominal valence of Tl should be Tl^{2+} . However, the doped atom Tl is known as a valence skipping element which takes Tl^{1+} [(6s)⁰ configuration] or Tl^{3+} [(6s)² configuration] but not Tl^{2+} , implying that (6s)¹ configuration is skipped even though a nominal valence is Tl^{2+} as in a series of compounds.²⁾ The logarithmic temperature dependence in the resistivity $\rho(T)$ in the low temperature region ($T < 10\text{K}$), which is robust against the magnetic field, and the occurrence of superconductivity were shown to be well explained on the basis of the negative- U Anderson model,³⁾ while fundamental properties of the negative- U Anderson model had already been derived in the beginning of 1990s.⁴⁾

Recently, it has been shown by the numerical renormalization group (NRG) calculation that the pair-hopping interaction U_{ph} between the localized electron and extended conduction electrons can give rise to the negative- U or valence skipping effect and the charge Kondo effect simultaneously.⁵⁾ More explicitly, it was shown that there exist two temperature (energy) scales T^* and T_K ($T_K < T^*$), with T_K being the Kondo temperature of the present problem, i.e., at $T < T^*$, (6s)¹ state is excluded (skipped) and (6s)⁰ and (6s)² states are degenerate or the negative- U effect manifests itself, and at

*miyake@toyotariken.jp

$T \lesssim T_K$, the charge Kondo effect occurs forming the charge singlet state, like the Kondo-Yosida spin singlet state. This origin of negative- U effect was new and quite different from a series of proposals which had already been given,⁶⁻¹¹⁾ while its origin still remains as an active subject.¹²⁾ Since there exists no magnetic ions in Tl doped PbTe, it is reasonable to expect that the two-fold charge degrees of freedom of Tl ion, Tl^{1+} and Tl^{3+} , is the origin of Kondo like behavior in the resistivity so that it was called the charge Kondo effect.^{1,3,4)}

Quite recently, temperature dependence of NMR relaxation rates $1/T_1T$ of ^{125}Te of $\text{Pb}_{1-x}\text{Tl}_x\text{Te}$ were reported to exhibit diverging increase below $T = 10$ K for the sample $x \simeq 0.01$ [ref. 13] which shows the charge Kondo effect in the resistivity and the superconductivity in the lower temperature region $T \lesssim T_K$.¹⁾ This is non-trivial because elements consisting of this compound are all non-magnetic ones, which suggests that the enhancement of $1/T_1T$ may give another smoking gun for the valence skipping or the negative- U effect to play a crucial role in this compound. It was also reported that the Knight shift of ^{125}Te is not influenced in the same temperature region, $T \sim T_K$, where the relaxation rate is enhanced. This is another mystery in the sense that the Korringa relation is apparently broken.

The purpose of the present paper is to clarify how the charge Kondo effect can give rise to the diverging behavior in $1/T_1T$ across the Kondo temperature T_K , reinforcing that the charge Kondo effect is the origin of anomalous properties observed in $\text{Pb}_{1-x}\text{Tl}_x\text{Te}$ ($0.006 < x < 0.015$). Organization of the paper is as follows. In Sect. 2, a formulation for discussing the relaxation rate $1/T_1T$ is given on the basis of the charge Kondo effect due to the pair-hopping interaction U_{ph} . In Sect. 3.1, it is shown the anomalous behaviors in the $1/T_1T$ arises from the first order process in the renormalized pair-hopping interaction $U_{\text{ph}}(T)$ by the charge Kondo effect at $T \gtrsim T_K$. In Sect. 3.2, it is also shown that the $1/T_1T$ is similarly influenced by the renormalized inter-orbital interaction $U_{\text{dc}}(T)$ between the localized electron and extended conduction electrons. As a result, it is shown in Sect. 3.3 that the anomalous temperature dependence of $1/T_1T$ observed in $\text{Pb}_{1-x}\text{Tl}_x\text{Te}$ ($x = 0.01$) is explained by these effects. On the other hand, in Sect. 4, it is shown that the charge Kondo effect does not influence the temperature dependence in the Knight shift at $T \sim T_K$ where the relaxation is enhanced by its effect. In Sect. 5, brief discussions are given on the temperature dependence in the $1/T_1T$ at $T_K \sim T \ll T^*$, and the difference in the relaxation rate $1/T_1T$ arising from the original (magnetic) Kondo effect.

2. Formulation

An effective model including the Coulomb interaction between the conduction electron and localized $6s$ orbital (denoted by d for manifesting the relation with the s - d model) is given as⁵⁾

$$\mathcal{H}_0 = \mathcal{H}_c + \mathcal{H}_d + \mathcal{H}_{\text{dc}} + \mathcal{H}_{\text{ph}} + \mathcal{H}_{\text{hyb}}, \quad (1)$$

where the first term is for the conduction electron, the second term is for 6s electrons, and the third and fourth terms are for the Coulomb interactions U_{dc} and the pair-hopping interaction U_{ph} between conduction electron and localized 6s electrons. Explicit expression of these terms are given as

$$\mathcal{H}_c \equiv \sum_{\mathbf{k}\sigma} \epsilon_{\mathbf{k}} c_{\mathbf{k}\sigma}^\dagger c_{\mathbf{k}\sigma}, \quad (2)$$

$$\mathcal{H}_d \equiv \epsilon_d \sum_{\sigma} n_{d\sigma}, \quad (3)$$

$$\mathcal{H}_{dc} \equiv U_{dc} \sum_{\mathbf{k}\sigma} c_{\mathbf{k}\sigma}^\dagger c_{\mathbf{k}\sigma} n_{d\sigma}, \quad (4)$$

$$\mathcal{H}_{ph} \equiv U_{ph} \sum_{\mathbf{k}\mathbf{k}'} \left(d_{\uparrow}^\dagger d_{\downarrow}^\dagger c_{\mathbf{k}\downarrow} c_{\mathbf{k}'\uparrow} + \text{h.c.} \right), \quad (5)$$

$$\mathcal{H}_{hyb} \equiv V_{dc} \sum_{\mathbf{k}\sigma} \left(c_{\mathbf{k}\sigma}^\dagger d_{\sigma} + \text{h.c.} \right), \quad (6)$$

where $n_{d\sigma} \equiv d_{\sigma}^\dagger d_{\sigma}$ is the number operator of the localized 6s electrons. Hereafter, the origin of energy is taken as the Fermi energy of conduction electrons ϵ_F , the chemical potential at $T = 0$, and the temperature T is assumed to be low enough compared to ϵ_F , i.e., $T \ll \epsilon_F$.

As discussed in Ref. 5, the pair-hopping interaction U_{ph} can stabilize the valence skipping state and cause the charge Kondo effect under certain condition. The origin of this phenomenon can be understood intuitively if we note that the U_{ph} is transformed to the pseudo-spin flipping exchange interaction (the origin of the Kondo effect) by the particle-hole transformation for the annihilation operators d_{\downarrow} and $c_{\mathbf{k}\downarrow}$ as shown explicitly in Appendix.

The NMR relaxation rate $1/T_1$ is given by the Moriya formula as¹⁴⁾

$$\frac{1}{T_1 T} = A^2 \frac{1}{\omega} \text{Im} \Gamma^R(\omega + i\delta), \quad (7)$$

where A is the hyper-fine coupling constant between electron and nuclei, and $\Gamma(i\omega_{\nu})$ is the transverse spin susceptibility of conduction electrons at certain Te site where NMR relaxation is observed and has several contributions, in general. The $\Gamma_{ph}(i\omega)$ arising from the lowest order process in U_{ph} is given by the Feynman diagram shown in Fig. 1 and its vertical inversion as follows:

$$\begin{aligned} \Gamma_{ph}(i\omega_{\nu}) &= 2V_{dc}^2 T^2 \sum_{\epsilon_n} U_{ph} G_c(\mathbf{r}_{ij}, i\epsilon_n) G_c(\mathbf{r}_{ij}, i\epsilon_n + i\omega_{\nu}) G_c(\mathbf{r}_{ij}, -i\epsilon_n) G_c(\mathbf{r}_{ij}, -i\epsilon_n + i\omega_{\nu}) \\ &\quad \times G_d(-i\epsilon_n + i\omega_{\nu}) G_d(i\epsilon_n), \end{aligned} \quad (8)$$

where we have used the property $G_c(-\mathbf{r}_{ij}, i\epsilon_n) = G_c(\mathbf{r}_{ij}, i\epsilon_n)$ etc., and the factor 2 arises from the diagrams of the vertical inversion. The expression [Eq. 8] is verified by the Wick decomposition as

$$\begin{aligned} &\left\langle T_{\tau} \left[\bar{c}_{i\uparrow}(\tau) c_{i\downarrow}(\tau) (-U_{ph}) \bar{d}_{i\uparrow}(\tau') \bar{d}_{i\downarrow}(\tau') c_{j\downarrow}(\tau') c_{j\uparrow}(\tau') \bar{c}_{i\downarrow}(\tau'') c_{i\uparrow}(\tau'') \right] \right\rangle \\ &= U_{ph} \langle T_{\tau} c_{j\uparrow}(\tau') \bar{c}_{i\uparrow}(\tau) \rangle \langle T_{\tau} c_{j\downarrow}(\tau') \bar{c}_{i\downarrow}(\tau'') \rangle \langle T_{\tau} c_{i\downarrow}(\tau) \bar{d}_{i\downarrow}(\tau') \rangle \langle T_{\tau} c_{i\uparrow}(\tau'') \bar{d}_{i\uparrow}(\tau') \rangle \end{aligned} \quad (9)$$

The reason why the Green functions with $\mp i\varepsilon_n$ and $\pm i\varepsilon_n + i\omega_\nu$ are paired in Fig. 1 is based on the fact that the Kondo-like renormalization enhancing the pair-hopping interaction U_{ph} arises for the annihilation process of pair of conduction electrons with $i\varepsilon_n$ and $-i\varepsilon_n$ as discussed in Appendix. Namely, the expression [Eq. (8)] is regarded as the most divergent part when U_{ph} divergently grows for the elastic scattering channel by the charge Kondo effect as decreasing temperature. This treatment of extracting the most divergent contribution is analogous to that adopted in the problem of estimating the effect of superconducting fluctuations to the conductivity near the superconducting transition point.^{15–17)} The renormalization of U_{ph} for a specified localized electron arises through the higher order terms in U_{ph} as in the conventional Kondo effect, and can be performed by the renormalization group (RG) method such as the poorman's scaling approach as discussed below.¹⁸⁾ On the other hand, the higher order terms in U_{ph} among different localized electrons are higher order in the impurity concentration and are safely neglected in the present case where the concentration of Tl impurity is small about 10^{-2} .

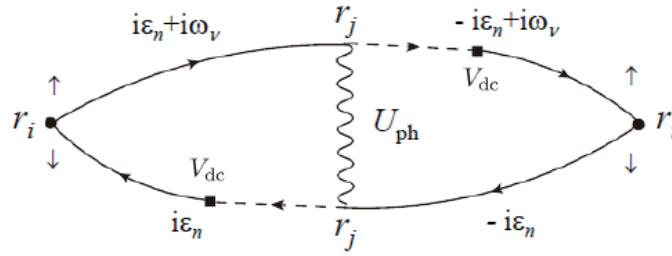


Fig. 1. Feynman diagram giving the NMR longitudinal relaxation rates $1/T_1T$ at Te (\mathbf{r}_i) site in the lowest order with respect to the pair-hopping interaction U_{ph} . Wavy line represents U_{ph} at Tl (\mathbf{r}_j) site. Solid lines with arrow and dashed lines with arrow represent the Matsubara Green function of conduction electrons of conduction band (in hole picture) and 6s electron at Tl site, respectively. Filled squares represent the hybridization V_{dc} between conduction electrons and 6s electron at Tl site.

As shown in Appendix, the Green function of the conduction electrons $G_c(\mathbf{r}, i\varepsilon_n)$ is expressed by a spectral representation as

$$G_c(\mathbf{r}, i\varepsilon_n) = \int_{-\infty}^{\infty} dy \frac{\rho(\mathbf{r}, y)}{i\varepsilon_n - y}, \quad (10)$$

with a spectral function

$$\rho(\mathbf{r}, y) = N_F \frac{e^{-(r/2\ell)}}{k_F r} \sin \left[\sqrt{\frac{y}{\epsilon_F} + 1} (k_F r) \right] \theta(y + \epsilon_F) \theta(\epsilon_c - y), \quad (11)$$

where $N_F \equiv mk_F/2\pi^2$ is the density of states of conduction electrons at the Fermi level, and ϵ_F and ϵ_c are the Fermi energy of conduction electrons and the energy cutoff of the conduction band in the hole (check) picture and a mean-free path due to the impurity scattering,²³⁾ respectively. In the limit

$k_F r \ll 1$, the spectral function takes a form as

$$\rho(\mathbf{r}, y) \approx \frac{mk_F}{2\pi^2} e^{-(r/2\ell)} \sqrt{\frac{y}{\epsilon_F} + 1} \theta(y + \epsilon_F) \theta(\epsilon_c - y). \quad (12)$$

The Green function of localized electron at valence-skipping site, i.e., T1 site, is given by

$$G_d(i\epsilon_n) = \frac{1}{i\epsilon_n - \epsilon_d} \quad (13)$$

where ϵ_d is the energy level of localized electron measured from the chemical potential.

3. NMR Relaxation Rate at $T \gtrsim T_K$

3.1 Effect of pair-hopping interaction

In this subsection, the NMR relaxation rate triggered by the pair-hopping interaction U_{ph} . As shown in Appendix, $\text{Im}\Gamma^{\text{R}}(\omega + i\delta)$ is given by

$$\begin{aligned} \text{Im}\Gamma_{\text{ph}}^{\text{R}}(\omega + i\delta) = & -\frac{2\pi V_{\text{dc}}^2 T U_{\text{ph}}}{\epsilon_d^2} \int_{-\infty}^{\infty} dy_4 \left[\text{th}\left(\frac{y_4 - \omega}{2T}\right) - \text{th}\frac{y_4}{2T} \right] \\ & \times \left[\rho(\mathbf{r}_{ij}, y_4 + \omega) \rho(\mathbf{r}_{ij}, -y_4 + \omega) G_c^{\text{R}}(\mathbf{r}_{ij}, -y_4) G_c^{\text{R}}(\mathbf{r}_{ij}, y_4) \right]. \end{aligned} \quad (14)$$

Therefore, to the leading order in ω and in the low temperature limit, $T \ll \epsilon_F$, $\text{Im}\Gamma^{\text{R}}(\omega + i\delta)/\omega$ is expressed in a compact form as

$$\frac{\text{Im}\Gamma_{\text{ph}}^{\text{R}}(\omega + i\delta)}{\omega} \approx \frac{4\pi V_{\text{dc}}^2 T U_{\text{ph}}}{\epsilon_d^2} \left[\rho(\mathbf{r}_{ij}, 0) G_c^{\text{R}}(\mathbf{r}_{ij}, 0) \right]^2. \quad (15)$$

With the use of definition Eq. (11) for the spectral function $\rho(\mathbf{r}, y)$, $\rho(\mathbf{r}, 0)$ is given by

$$\rho(\mathbf{r}, 0) = N_F \frac{e^{-(r/2\ell)}}{k_F r} \sin(k_F r), \quad (16)$$

and an explicit form of $G_c^{\text{R}}(\mathbf{r}, \epsilon)$ is given by

$$G_c^{\text{R}}(\mathbf{r}, \epsilon) = N_F \frac{e^{-(r/2\ell)}}{k_F r} \int_{-\epsilon_F}^{\epsilon_c} dy \sin \left[\sqrt{\frac{y}{\epsilon_F} + 1} (k_F r) \right] \frac{1}{\epsilon - y}. \quad (17)$$

Therefore, $G_c^{\text{R}}(\mathbf{r}, 0)$ is expressed as

$$G_c^{\text{R}}(\mathbf{r}, 0) = -N_F e^{-(r/2\ell)} J(k_F r), \quad (18)$$

with a function defined as

$$J(k_F r) \equiv \frac{1}{k_F r} \int_{-\epsilon_F}^{\epsilon_c} dy \sin \left[\sqrt{\frac{y}{\epsilon_F} + 1} (k_F r) \right] \frac{1}{y}. \quad (19)$$

The result of numerical integration in Eq. (19) is shown in Fig. 2 for a series of (ϵ_c/ϵ_F) s.

Substituting Eqs. (16) and (17) into Eq. (15), the NMR relaxation rate $(1/T_1 T)_{\text{ph}}$ [Eq. (7)] in the low temperature limit ($T \ll \epsilon_F$) is given by

$$\left(\frac{1}{T_1 T} \right)_{\text{ph}} \approx A^2 \frac{4\pi (V_{\text{dc}} N_F^2)^2 T U_{\text{ph}}}{\epsilon_d^2} e^{-(r/\ell)} \left[\frac{\sin(k_F r)}{k_F r} J(k_F r) \right]^2. \quad (20)$$

This formula offers the basis for discussing anomalous enhancement of the relaxation rate $1/T_1 T$ in

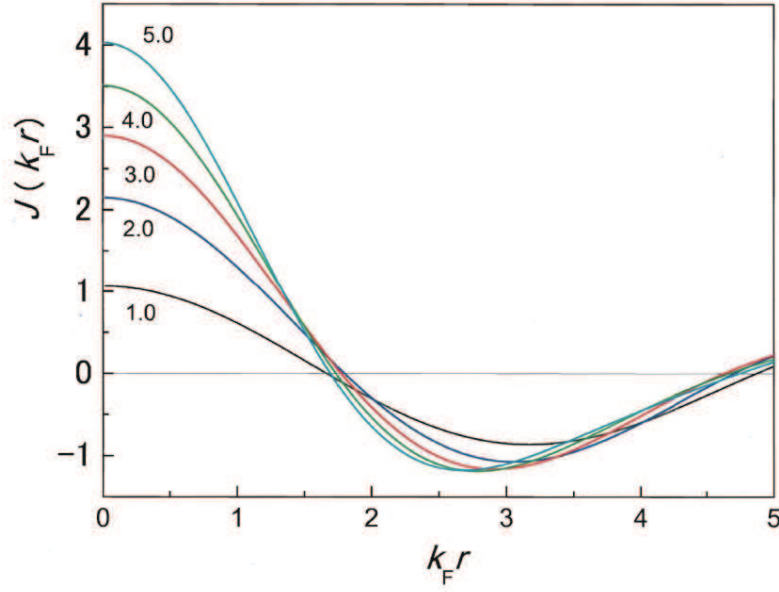


Fig. 2. $J(k_F r)$ for a series of (ϵ_c/ϵ_F) s.

the region $T \gtrsim T_K$.

In the limit $k_F r \ll 1$, the integration with respect to y in Eq. (19) is given by

$$J(k_F r) \simeq 2 \sqrt{\frac{\epsilon_F}{\epsilon_c} + 1} + \log \left| \frac{\sqrt{\epsilon_c + \epsilon_F} - \sqrt{\epsilon_F}}{\sqrt{\epsilon_c + \epsilon_F} + \sqrt{\epsilon_F}} \right|, \quad (21)$$

as shown in Appendix. On the other hand, in the limit $k_F r \gg 1$, the asymptotic form of $J(k_F r)$ is given as

$$J(k_F r) \approx \frac{1}{k_F r} \pi \cos(k_F r), \quad (22)$$

as shown in Appendix. Note that the asymptotic form shown in Fig. 2 is consistent with the result [Eq. (22)]. Therefore, in the limit $k_F r \gg 1$, $1/T_1 T$ given by Eq. (20) is in proportion to $e^{-(r/\ell)} [\sin(2k_F r)/(k_F r)^2]^2$.

According to the result based on the NRG calculation,⁵⁾ the renormalized pair-hopping interaction U_{ph} , owing to the impurity charge Kondo effect, is expected to exhibit a diverging T dependence as T decreases. This is because, as shown in Appendix, the U_{ph} is transformed to the spin exchange interaction by the particle-hole transformation for the down spin component of both localized (d) and conduction electrons, so that it is enhanced in parallel to the magnetic Kondo effect. Indeed, the renormalization of U_{ph} up to the second order in U_{ph} and U_{dc} is given by the Feynman diagrams shown in Fig. 3(a). Similarly, that of U_{dc} is given by the Feynman diagram shown in Fig. 3(b). These processes are formally the same as those appearing the magnetic Kondo problem because U_{ph} and U_{dc} correspond to $J_{\perp}/2$ and $J_z/4$ in the anisotropic s-d model, respectively, in the mapped world by the

transformations [Eqs. (A·1) and (A·2)] as discussed in Appendix.

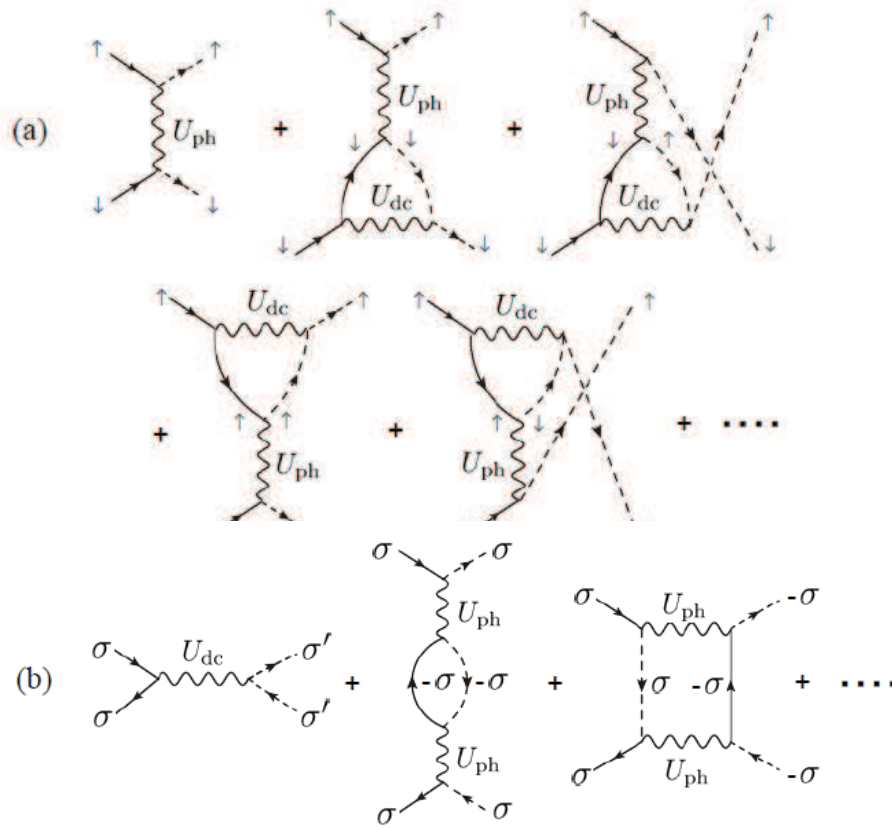


Fig. 3. Feynman diagram for the renormalization of (a) the pair-hopping interaction U_{ph} and (b) the inter-orbital interaction U_{dc} , up to the second order in U_{ph} and U_{dc} . These are formally the same as those in the anisotropic s-d model.

In order to take into account a series of higher order corrections with respect to U_{ph} and U_{dc} , it is useful to rely on RG approaches in general. Here, we adopt the one-loop order (or poorman' scaling) approximation.¹⁸⁾ As shown in Appendix [Eq. (G·8)], the T dependent renormalized pair-hopping interaction $U_{\text{ph}}(T)$ [$\equiv y_{\perp}(T)/2N_{\text{F}}$] is given as

$$U_{\text{ph}}(T) = \frac{1}{2N_{\text{F}} \log(T/T_{\text{K}})}, \quad (23)$$

and has the logarithmic T dependence, in the high temperature region at $T \gtrsim T_{\text{K}}$, like

$$U_{\text{ph}}(T) \approx U_{\text{ph}}^0 - 4N_{\text{F}} U_{\text{ph}}^0 U_{\text{dc}}^0 \log \frac{T}{E_{\text{c}}^0}, \quad (24)$$

where U_{ph}^0 and U_{dc}^0 are the bare pair-hopping and inter-orbital interactions, respectively, and E_{c}^0 is the bare bandwidth of conduction electrons. On the other hand, $U_{\text{ph}}(T)$ exhibits divergent behavior toward $T = T_{\text{K}}$ as $U_{\text{ph}}(T) \approx U_{\text{ph}}^0 / \log(T/T_{\text{K}})$ in the one-loop order RG approximation. Replacing U_{ph}

in Eq. (20) by $U_{\text{ph}}(T)$ [Eq. (23)], the NMR relaxation rates $(1/T_1T)_{\text{ph}}$ at Te site (\mathbf{r}) is given by

$$\left(\frac{1}{T_1T}\right)_{\text{ph}} \approx A^2 \frac{4\pi(V_{\text{dc}}N_{\text{F}})^2}{\epsilon_{\text{d}}^2} e^{-(r/\ell)} \left[\frac{\sin(k_{\text{F}}r)}{k_{\text{F}}r} J(k_{\text{F}}r) \right]^2 T U_{\text{ph}}(T). \quad (25)$$

The procedure of replacing the bare pair-hopping interaction U_{ph}^0 by the renormalized one $U_{\text{ph}}(T)$ may be justified by the expression [Eq. (14)] in which major contribution comes from the conduction electrons with the energy $y_4 \lesssim T$. Equation (25) is one of central results of the present paper. Namely, the NMR relaxation rates $1/T_1T$ at Te sites near the Tl site should exhibit pronounced increase as T decreases toward the Kondo temperature T_{K} of the charge Kondo effect. This result is a signature of the diverging increase in the NMR relaxation rate $1/T_1T$ of ^{125}Te of $\text{Pb}_{1-x}\text{Tl}_x\text{Te}$ observed below $T = 10$ K for the sample $x \simeq 0.01$ in Ref. 13. The result is expected to remain essentially valid if we adopt more solid calculations, such as the NRG calculation,⁵⁾ because the diverging behavior in the renormalized pair-hopping interaction U_{ph} toward $T = T_{\text{K}}$ is still expected as discussed in the end of the present section.

Concluding this subsection, it should be remarked that there exist higher order corrections in U_{ph} to the diagram shown in Fig. 1 which is essentially independent of the Kondo-like renormalization on the pair-hopping interaction U_{ph} itself given by the vertical processes shown in Fig. 3(a). For example, such a next order correction $\Delta U_{\text{ph}}(i\omega_{\nu})$ to U_{ph} in Fig. 1 (in the horizontal direction) is given by Fig. 4 whose analytic expression is

$$\begin{aligned} \Delta U_{\text{ph}}(i\omega_{\nu}) &= -U_{\text{ph}}^2 T \sum_{\epsilon_{n''}} G_{\text{d}}(i\epsilon_{n''} + i\omega_{\nu}) G_{\text{d}}(-i\epsilon_{n''}) \\ &= -U_{\text{ph}}^2 \frac{1}{2\epsilon_{\text{d}} - i\omega_{\nu}} \tanh\left(\frac{\epsilon_{\text{d}}}{2T}\right), \end{aligned} \quad (26)$$

where the minus sign arises from the order of perturbation expansion with respect to U_{ph} compared to the first order term in U_{ph} given by Fig. 1. After analytic continuation $i\omega_{\nu} \rightarrow \omega + i\delta$, $\Delta U_{\text{ph}}^{\text{R}}(\omega + i\delta)$ is reduced to

$$\Delta U_{\text{ph}}^{\text{R}}(\omega + i\delta) = -U_{\text{ph}}^2 \frac{1}{2\epsilon_{\text{d}}} \tanh\left(\frac{\epsilon_{\text{d}}}{2T}\right), \quad (27)$$

where we have used the relation $\delta(\omega - \epsilon_{\text{d}}) = 0$ which holds at $\omega \sim 0$. This correction is negative and gives the suppression of the effect of the pair-hopping interaction in contrast to the enhancement by the Kondo-like renormalization given by the vertical processes shown in Fig. 3. This kind of counter renormalization effect is a general aspect of the Kondo effect in which the effect of the divergent increase of the effective exchange coupling constant J finally becomes inactive because of the Kondo-Yosida singlet formation^{24,25)} by the divergent exchange coupling constant itself.¹⁸⁾ Indeed, it was demonstrated that the vertex correction for the spin susceptibility is crucial to obtain the Korringa relation characteristic of the local Fermi liquid property in multi orbital d-electron impurity Anderson

model.²⁷⁾ However, such an effect of renormalization becomes crucial only at $T < T_K$ where the Kondo-Yosida singlet state is formed. Therefore, it plays minor roles in the region $T \gtrsim T_K$ where the diverging T dependence in $1/T_1T$ is observed.

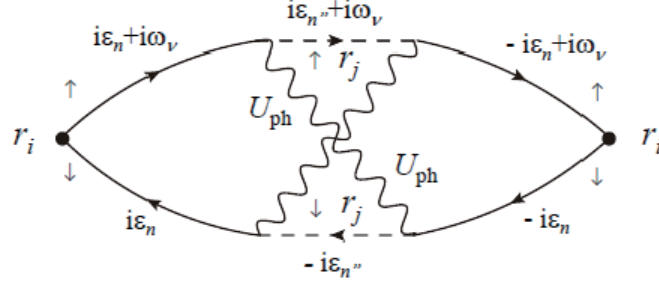


Fig. 4. Feynman diagram giving the NMR longitudinal relaxation rates $1/T_1T$ at Te (\mathbf{r}_i) site in the second order in the pair-hopping interaction U_{ph} . Notations are the same as those of Fig. 1

3.2 Effect of inter-orbital interaction

In this subsection, the NMR relaxation rate triggered by the inter-orbital interaction U_{dc} . Although it was demonstrated that the pair-hopping interaction U_{ph} enhances the NMR relaxation rate toward $T = T_K$, it is crucial to note that the inter-orbital interaction U_{dc} is also renormalized (enhanced) by the charge Kondo effect, as shown in Appendix [Eq. (G-9)], and the T dependent $U_{dc}(T)$ also has the logarithmic T dependence in the high temperature region $T \gtrsim T_K$ as

$$U_{dc}(T) \approx U_{dc}^0 - N_F(U_{ph}^0)^2 \log \frac{T}{E_c}, \quad (28)$$

and exhibits divergent behavior toward $T = T_K$ as $U_{dc}(T) \approx 1/[4N_F \log(T/T_K)]$ in the one-loop order RG approximation, like in Eq. (23) as shown in Appendix . Therefore, we have to keep the relaxation processes caused by the effect of U_{dc} . There are three types of processes causing the relaxation in the first order in U_{dc} . One of them is given by the Feynman diagram shown in Fig. 5 or its vertical inversion. This is a type of vertex correction to the local magnetic susceptibility of conduction electrons at certain Te site. Corresponding to the expression [Eq. (8)], the analytic expression for the function $\Gamma_{dcV}(i\omega_v)$ for this correction is given by

$$\Gamma_{dcV}(i\omega_v) = \frac{2V_{dc}^2}{\epsilon_d^2} T^2 \sum_{\epsilon_n} U_{dc} \left[G_c(\mathbf{r}_{ij}, i\epsilon_n) G_c(\mathbf{r}_{ij}, i\epsilon_n + i\omega_v) \right]^2, \quad (29)$$

where we have used the property $G_c(-\mathbf{r}_{ij}, i\epsilon_n) = G_c(\mathbf{r}_{ij}, i\epsilon_n)$ etc., and the factor 2 arises from the diagram of the vertical inversion.

Other types of processes causing the relaxation are given by the Feynman diagrams shown in Figs. 6(a) and (b) and Figs. 7(a) and (b). These are a type of the self-energy corrections to the conduction

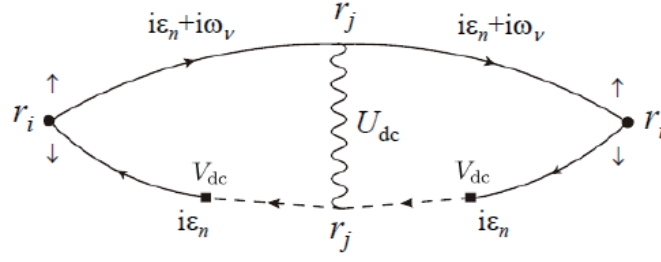


Fig. 5. Feynman diagram giving the NMR longitudinal relaxation rates $1/T_1T$ at Te (\mathbf{r}_i) site in the lowest order with respect to the inter-orbital interaction U_{dc} which corresponds to that given by Fig. 1. Other notations are the same as in Fig. 1.

electrons. It is easy to see that the contribution from Figs. 7(a) and (b) are twice of that from Figs. 6(a) and (b), due to spin degrees of freedom, with negative sign due to the extra Fermion-loop factor (-1) . Therefore, the analytic expression for the function $\Gamma_{dcS}(i\omega_v)$ corresponding to diagrams shown in Figs. 6(a) and (b) and Figs. 7(a) and (b) is given as

$$\Gamma_{dcS}(i\omega_v) = -\frac{2V_{dc}^2}{\epsilon_d^2} T^2 \sum_{\epsilon_n} U_{dc} \left\{ [G_c(\mathbf{r}_{ij}, i\epsilon_n)]^2 G_c(0, i\epsilon_n) G_c(0, i\epsilon_n - i\omega_v) [G_d(i\epsilon_n)]^2 + [G_c(\mathbf{r}_{ij}, i\epsilon_n)]^2 G_c(0, i\epsilon_n) G_c(0, i\epsilon_n + i\omega_v) [G_d(i\epsilon_n)]^2 \right\}, \quad (30)$$

where the first and second terms are for the Figs. 6(a) and (b), respectively, and the factor 2 arises from the diagrams of the mirror inversion.

Performing calculations similar to that obtaining the expression Eq. (14) for $\text{Im}\Gamma_{ph}^R(\omega + i\delta)$, the expression of $\text{Im}\Gamma_{dcV}^R(\omega + i\delta)$ is given, to the leading order in ω , as

$$\text{Im}\Gamma_{dcV}^R(\omega + i\delta) = -\frac{4\pi\omega V_{dc}^2 T U_{dc}}{\epsilon_d^2} \int_{-\infty}^{\infty} dy \frac{\partial}{\partial y} \left(\text{th} \frac{y}{2T} \right) [\rho(\mathbf{r}_{ij}, y) G_c^R(\mathbf{r}_{ij}, y)]^2. \quad (31)$$

Then, in the low temperature limit ($T \ll \epsilon_F$), the $\text{Im}\Gamma_{dcV}^R(\omega + i\delta)/\omega$ is reduced to a compact form as

$$\frac{\text{Im}\Gamma_{dcV}^R(\omega + i\delta)}{\omega} \approx -\frac{8\pi V_{dc}^2 T U_{dc}}{\epsilon_d^2} [\rho(\mathbf{r}_{ij}, 0) G_c^R(\mathbf{r}_{ij}, 0)]^2. \quad (32)$$

This term has the same form as Eq. (15) giving $\text{Im}\Gamma_{ph}^R(\omega + i\delta)/\omega$ with U_{ph} being replaced by $-U_{dc}$. Therefore, it has an effect that U_{ph} in Eq. (15) is replaced by $(U_{ph} - 2U_{dc})$.

Similarly, the expression of $\text{Im}\Gamma_{dcS}^R(\omega + i\delta)$ is given, to the leading order in ω , as

$$\text{Im}\Gamma_{dcS}^R(\omega + i\delta) = \frac{2\pi\omega V_{dc}^2 T U_{dc}}{\epsilon_d^2} \int_{-\infty}^{\infty} dy_3 \frac{\partial}{\partial y_3} \left(\text{th} \frac{y_3}{2T} \right) [\rho(0, y_3) G_c^R(\mathbf{r}_{ij}, y_3)]^2. \quad (33)$$

Here, we have left only the contribution from the energy conservation processes of particle-hole pairs of conduction electrons between the site of localized d state (associated with the Fock type process) and free conduction electrons. Such a contribution arises from the combination of $G_c(0, i\epsilon)$ and

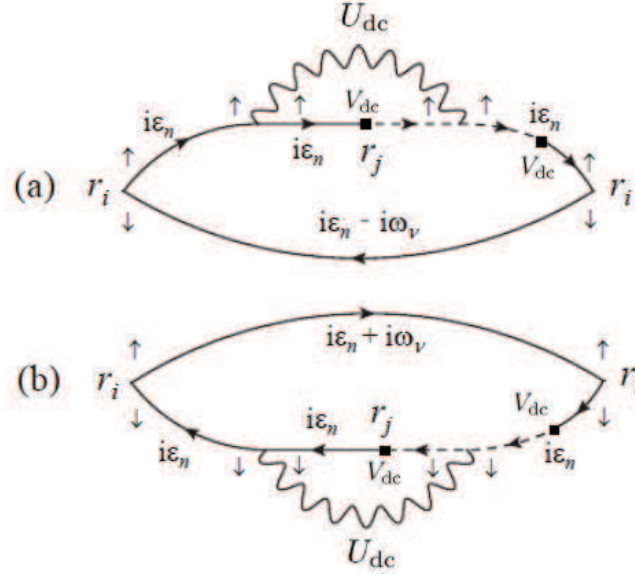


Fig. 6. Feynman diagram giving the NMR longitudinal relaxation rates $1/T_1T$ at Te (\mathbf{r}_i) site in the lowest order with respect to the inter-orbital interaction U_{dc} which corresponds to a Fock type self-energy correction. Other notations are the same as in Fig. 1.

$G_c(0, i\varepsilon \pm i\omega_v)$ in the expression Eq. (C·8). On the other hand, we have discarded contributions arising from the combination of $G_c(\mathbf{r}_{ij}, i\varepsilon)$ and $G_c(0, i\varepsilon \pm i\omega_v)$ in which the inter-orbital interaction U_{dc} works to renormalize the local level of conduction electrons at the site of localized d state, because the level shift of conduction electrons there could be absorbed in the chemical potential that should be maintained as constant in space. In the same sense, we have not taken into account the contribution from Feynman diagram that is obtained by replacing a closed loop in Figs. 7(a) by that of purely the localized d electron. This procedure of calculation is based on the physical picture similar to that behind the Thomas-Fermi screening argument in which the number density of conduction electrons changes so as to maintain the chemical potential as uniform in space even though the energy level of the conduction electrons is modified by the external electric charge.¹⁹⁾ The validity of this way of calculation is also reinforced by the fact the latter contributions vanish in the case of uniform system in which the wave vector representation can be used.

Then, in the low temperature limit ($T \ll \epsilon_F$), the $\text{Im}\Gamma_{dcS}^R(\omega + i\delta)/\omega$ [Eq. (33)] is reduced to a compact form as

$$\frac{\text{Im}\Gamma_{dcS}^R(\omega + i\delta)}{\omega} \approx \frac{4\pi V_{dc}^2 T U_{dc}}{\epsilon_d^2} \left[\rho(0, 0) G_c^R(\mathbf{r}_{ij}, 0) \right]^2. \quad (34)$$

Substituting the expressions for $\rho(0, 0)$ [Eq. (16)] and $G_c^R(\mathbf{r}_{ij}, 0)$ [Eq. (18)] and replacing the bare inter-orbital interaction U_{dc}^0 by the renormalized one, $U_{dc}(T)$ [Eq. (G·9)], the relaxation rate $(1/T_1T)_{dcS}$ [Eq.

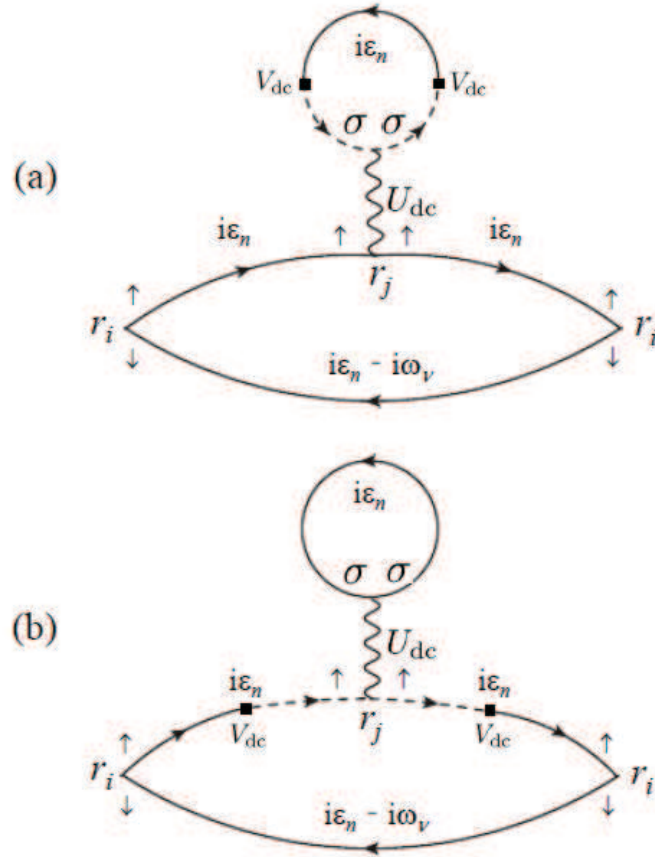


Fig. 7. Feynman diagram giving the NMR longitudinal relaxation rates $1/T_1T$ at Te (r_i) site in the lowest order with respect to the inter-orbital interaction U_{dc} which corresponds to a Hartree type self-energy correction. The summation with respect to spin component $\sigma = \uparrow$ and \downarrow . Other notations are the same as in Fig. 1.

(7)] is given as

$$\left(\frac{1}{T_1T}\right)_{dcS} \approx A^2 \frac{4\pi(V_{dc}N_F)^2}{\epsilon_d^2} e^{-(r/\ell)} [J(k_F r)]^2 T U_{dc}(T). \quad (35)$$

This formula is another central results of the present paper and offers us the basis for discussing anomalous behavior of the relaxation rate $1/T_1T$ in the region $T \sim T_K$.

3.3 Short summary for NMR relaxation rate

The total relaxation rate ($1/T_1T$) is given by the sum of ($1/T_1T$)_{ph} [Eq. (25)], ($1/T_1T$)_{dcV} [Eq. (32)], and ($1/T_1T$)_{dcS} [Eq. 35)] as follows:

$$\frac{1}{T_1T} \approx A^2 \frac{4\pi(V_{dc}N_F)^2}{\epsilon_d^2} e^{-(r/\ell)} \left[\frac{\sin(k_F r)}{k_F r} J(k_F r) \right]^2 T [U_{ph}(T) - 2U_{dc}(T)]$$

$$+A^2 \frac{4\pi(V_{\text{dc}}N_{\text{F}})^2}{\epsilon_{\text{d}}^2} e^{-(r/\ell)} [J(k_{\text{F}}r)]^2 T U_{\text{dc}}(T), \quad (36)$$

where we have used back the expressions of $U_{\text{ph}}(T)$ [Eq. (G·8)] and $U_{\text{dc}}(T)$ [Eq. (G·9)]. Since U_{ph} and U_{dc} correspond to $J_{\perp}/2$ and $J_z/4$, respectively, as discussed in Appendices and , the ratio of $[U_{\text{ph}}(T) - 2U_{\text{dc}}(T)]$ in the first term of Eq. (36) and $U_{\text{ph}}(T)$ approaches zero toward $T = T_{\text{K}}$ as decreasing temperature. Therefore, the first term gives less divergent behavior compared to the second term. On the other hand, the second term in Eq. (36) exhibits pronounced increase as T decreases, toward $T = T_{\text{K}}$ from the region $T \gtrsim T_{\text{K}}$, through the T dependence of $TU_{\text{dc}}(T)$ (in dimensionless form) shown in Fig. 8 in which the T dependence of $U_{\text{dc}}(T)$ is given by the one-loop order RG (or poorman's scaling) approximation as

$$U_{\text{dc}}(T) = \frac{1}{4N_{\text{F}} \log \frac{T}{T_{\text{K}}}}. \quad (37)$$

(See Eq. (G·10) for y_z and definition of $U_{\text{dc}}(E) \equiv y_z/4N_{\text{F}}$ in Appendix). Of course, the result of poorman's scaling ceases to be valid very near $T = T_{\text{K}}$. Nevertheless, it would give an increasing tendency of $TU_{\text{dc}}(T)$ around $T = T_{\text{K}}$. The dotted line in Fig. 8 shows an expected T dependence of $TU_{\text{dc}}(T)$ at $T \lesssim T_{\text{K}}$, which is reasonable considering that the increasing tendency of $TU_{\text{dc}}(T)$ already begins to appear at $T \simeq 2.7T_{\text{K}}$, i.e., from far higher temperature than T_{K} , and that the divergent T dependence in $U_{\text{dc}}(T)$ at $T \ll T_{\text{K}}$ works to suppress the Curie like divergence ($\propto 1/T$) of localized electron when entering into the local Fermi liquid state²⁶⁾ in which the Kondo-Yosida charge singlet state is formed as in the case of magnetic Kondo problem.²⁷⁾ Since the *divergent* part in $1/T_1T$ [Eq. (36)] is in proportion to $TU_{\text{dc}}(T)$, this theoretical result for $1/T_1T$ qualitatively explains the anomalous temperature dependence of $1/T_1T$ observed in $\text{Pb}_{1-x}\text{Tl}_x\text{Te}$ ($x \simeq 0.01$) reported by Ref. 13. However, of course to obtain quantitative result for the T dependence in $1/T_1T$ at $T \lesssim T_{\text{K}}$, we need perform more solid calculations, such as numerical renormalization group method,⁵⁾ which is left for future study.

Concluding this section, it is remarked that the present relaxation mechanism is quite different from the case of magnetic Kondo impurity in which $1/T_1T$ is essentially in proportion to J_{\perp}^2 as discussed in Ref. 20. This difference is traced back to the difference in the order of perturbation process giving the relaxation rates. In the present case, $1/T_1T$ is given by the first order process in the pair-hopping interaction U_{ph} and the inter-orbital interaction U_{dc} , while that in the case of magnetic Kondo impurity is given by the second order process in the s-d exchange interaction J_{\perp} causing the spin-flip process, as discussed in Ref. 20

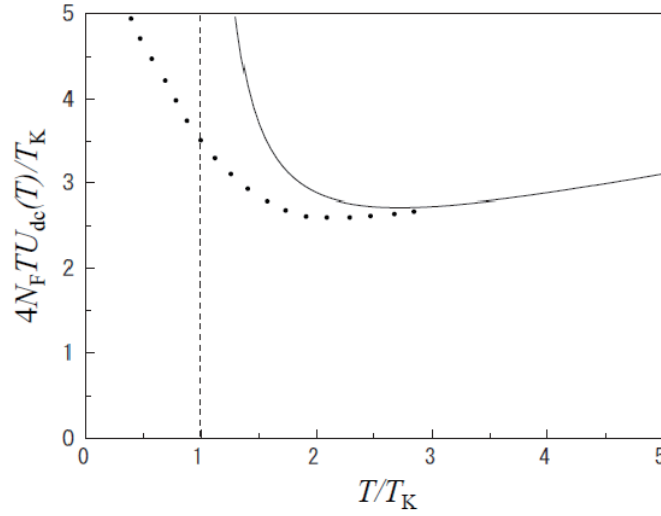


Fig. 8. $4N_F T U_{dc}(T)/T_K$ vs T/T_K with T_K being the Kondo temperature in the one-loop order RG (poorman's scaling) approximation [Eq. (D·2)]. Dotted line is a guide to the eyes for a qualitative behavior expected in exact treatment beyond poorman's scaling solution as discussed in the text.

4. Knight Shift at $T \gtrsim T_K$

One probably tends to expect that the anomalous behavior in the relaxation rate $1/T_1 T$ discussed in the previous section should be manifested also in the Knight shift. However, this is not the case as discussed below. The lowest order contribution to the Knight shift with respect to the inter-orbital interaction U_{dc} arises from the process given by the Feynman diagram shown in Fig. 9 and its mirror inversion with respect to U_{dc} where we have retained only the elastic scattering processes without change of the Matsubara frequencies following the argument justifying the distribution of the Matsubara frequencies in Fig. 1. We have also discarded the type of processes of selfenergy correction of conduction electrons because these effect is absorbed in the chemical potential as discussed in Sect. 3.2. Note that the pair-hopping interaction U_{ph} does not contribute to the the Knight shift because the U_{ph} is associated with spin-flip processes of conduction electrons.

In parallel to the expression of the relaxation rate [Eq. (7)], the extra contribution to Knight shift ΔK from the charge Kondo effect is given by

$$\Delta K = A \frac{1}{2} \text{Re} [\chi_{\uparrow\uparrow}^R(\mathbf{r}_{ij}, i\delta) - \chi_{\uparrow\downarrow}^R(\mathbf{r}_{ij}, i\delta)], \quad (38)$$

where $\chi_{\sigma\sigma'}^R(\mathbf{r}_{ij}, \omega + i\delta)$ is the retarded function of $\chi_{\sigma\sigma'}(i\omega_\nu)$ given by the Feynman diagram shown in Fig. 9 and its mirror inversion with respect to U_{dc} . Its explicit form is given as follows:

$$\chi_{\sigma\sigma'}(\mathbf{r}_{ij}, i\omega_\nu) = -2V_{dc}^2 M_{\sigma\sigma'}(\mathbf{r}_{ij}, i\omega_\nu) \quad (39)$$

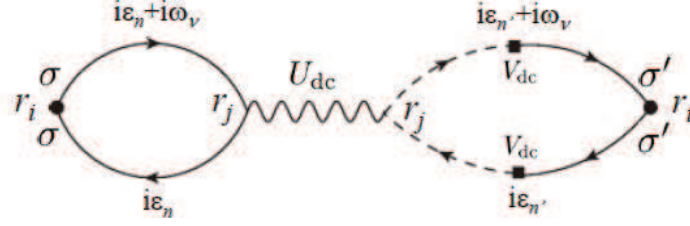


Fig. 9. Feynman diagram giving one of the responses that is diagonal in spin space in the lowest order process in U_{dc} . The other diagram is that given by mirror inversion with respect to U_{dc} .

where the minus sign arises from the factor (+1) reflecting even number of exchanges of fermion operators in the Wick theorem giving a factor (+1) and the (-1) associated with the first order perturbation, and $M_{\uparrow\uparrow}(\mathbf{r}_{ij}, i\omega_\nu)$ is defined by

$$M_{\sigma\sigma'}(\mathbf{r}_{ij}, i\omega_\nu) \equiv T^2 \sum_{\varepsilon_n, \varepsilon_{n'}} U_{dc} G_c(\mathbf{r}_{ij}, i\varepsilon_n) G_c(\mathbf{r}_{ij}, i\varepsilon_n + i\omega_\nu) G_c(\mathbf{r}_{ij}, i\varepsilon_{n'}) G_c(\mathbf{r}_{ij}, i\varepsilon_{n'} + i\omega_\nu) \times G_d(i\varepsilon_{n'} + i\omega_\nu) G_d(i\varepsilon_{n'}). \quad (40)$$

where we have used the property $G_c(-\mathbf{r}_{ij}, i\varepsilon_n) = G_c(\mathbf{r}_{ij}, i\varepsilon_n)$ etc. The expression [Eq. 40] is verified by the Wick decomposition for $M_{\uparrow\downarrow}$ as

$$\begin{aligned} & \langle T_\tau \left[\bar{c}_{i\uparrow}(\tau) c_{i\uparrow}(\tau) (-U_{dc}) \bar{d}_{i\downarrow}(\tau') \bar{d}_{i\downarrow}(\tau') \bar{c}_{j\uparrow}(\tau') c_{j\uparrow}(\tau') \bar{c}_{i\downarrow}(\tau'') c_{i\downarrow}(\tau'') \right] \rangle \\ &= -U_{dc} \langle T_\tau c_{i\uparrow}(\tau) \bar{c}_{j\uparrow}(\tau') \rangle \langle T_\tau c_{i\uparrow}(\tau) \bar{c}_{j\uparrow}(\tau') \rangle \langle T_\tau c_{i\uparrow}(\tau'') \bar{d}_{i\uparrow}(\tau') \rangle \langle T_\tau d_{i\uparrow}(\tau') \bar{c}_{i\uparrow}(\tau'') \rangle, \end{aligned} \quad (41)$$

and the expression [Eq. 40] is verified by the Wick decomposition $M_{\uparrow\uparrow}$ as

$$\begin{aligned} & \langle T_\tau \left[\bar{c}_{i\uparrow}(\tau) c_{i\uparrow}(\tau) (-U_{dc}) \bar{d}_{i\uparrow}(\tau') \bar{d}_{i\uparrow}(\tau') \bar{c}_{j\uparrow}(\tau') c_{j\uparrow}(\tau') \bar{c}_{i\uparrow}(\tau'') c_{i\uparrow}(\tau'') \right] \rangle \\ &= -U_{dc} \langle T_\tau c_{i\uparrow}(\tau) \bar{c}_{j\uparrow}(\tau') \rangle \langle T_\tau c_{i\uparrow}(\tau) \bar{c}_{j\uparrow}(\tau') \rangle \langle T_\tau c_{i\downarrow}(\tau'') \bar{d}_{i\downarrow}(\tau') \rangle \langle T_\tau d_{i\downarrow}(\tau') \bar{c}_{i\downarrow}(\tau'') \rangle. \end{aligned} \quad (42)$$

Note that $M_{\sigma\sigma'}(\mathbf{r}_{ij}, i\omega_\nu)$ is independent both of σ and σ' . Therefore, the correction to the Knight shift [Eq. (38)] cancels as far as the diverging term through the renormalization of $U_{dc}(T)$ is concerned, in contrast to the case of the relaxation rate $1/T_1 T$ which shows sharp increase in the temperature region $T \gtrsim T_K$. This result is reasonable considering that the two configurations of localized electrons, $(6s)^0$ and $(6s)^2$, are both magnetically inert so that they give no *static* effect on the surrounding conduction electrons, which is consistent with experimental observation.¹³⁾ In this sense, the so-called Korringa relation is apparently broken.

It is interesting to note that such breaking down of the Korringa relation is also realized in f^2 -based heavy fermion metals with a singlet crystalline-electric-field ground state such as UPt_3 .^{28,29)} Indeed, in UPt_3 , the Knight shift decrease across the the superconducting transition is not enhanced but is

comparable to that of Pr metals,³⁰⁾ while the relaxation rate $1/T_1$ is highly enhanced in accordance with the mass enhancement observed in the specific heat measurement.³¹⁾ The physical interpretation of this phenomenon is as follows: The enhancement in the effective mass of the quasiparticles of f^1 state is compensated by the probability of making such f^1 states by breaking the f^2 singlet crystalline-electric-field ground state, leading to the unenhanced magnetic susceptibility, while the relaxation process of existing magnetization caused by quasiparticles polarization is free from such a compensation.

On the other hand, the local charge susceptibility $\chi_{\text{charge}} = 2[\chi_{\uparrow\uparrow}^R(\mathbf{r}_{ij}, i\delta) + \chi_{\uparrow\downarrow}^R(\mathbf{r}_{ij}, i\delta)]$ is given by

$$\chi_{\text{charge}} = -4V_{\text{dc}}^2 T^2 \sum_{\varepsilon_n, \varepsilon_{n'}} U_{\text{dc}} \left[G_c(\mathbf{r}_{ij}, i\varepsilon_n) \right]^2 \left[G_c(\mathbf{r}_{ij}, i\varepsilon_{n'}) G_d(i\varepsilon_{n'}) \right]^2, \quad (43)$$

and is subject to the suppression through the enhancement of U_{dc} by the charge Kondo effect because the summand with respect to ε_n is even in ε_n and is not vanishing but remaining a positive value in the limit $\varepsilon_n \rightarrow 0$. Note that, in the mapped world by the transformations [Eqs. (A-1) and (A-2)] (as discussed in Appendix), the U_{dc} corresponds to $J_z/4$ in the anisotropic s-d model, so that the U_{dc} is enhanced together with U_{ph} by the charge Kondo effect as explicitly shown in Appendix.⁶⁾ Therefore, the charge susceptibility χ_{charge} is suppressed by the charge Kondo effect. This result is physically reasonable considering that the repulsive Coulomb inter-orbital interaction U_{dc} should work to suppress the charge fluctuation in general. It can be confirmed experimentally in principle in one form or another.

5. Summary

We have shown that the anomalous NMR response observed in $\text{Pb}_{1-x}\text{Tl}_x\text{Te}$ ($x \sim 0.01$) can be explained by the charge Kondo effect which is caused by the pair-hopping interaction U_{ph} and the inter-orbital interaction U_{dc} between localized orbital on Tl and conduction electrons doped in the semiconductor PbTe. Sharp increase observed in the NMR relaxation rate $1/T_1 T$ of ^{125}Te at $T < 10\text{K}$ can be understood essentially as the increase of U_{ph} and U_{dc} due to Kondo-like renormalization in the region $T \gtrsim T_K$ because U_{ph} and U_{dc} can mediate the spin-flip of conduction electrons as shown in Fig. 1, and Figs. 5, 6, and 7, respectively. We have also shown that the normal behavior of the Knight shift K at the same temperature region $T < 10\text{K}$ can be understood on the same formalism because U_{ph} does not mediate the diagonal response of the spin susceptibility and the effect of U_{dc} cancels in the spin susceptibility, although U_{dc} exhibits divergent increase toward $T = T_K$ together with U_{ph} . In this sense, the Korringa relation is apparently broken in the system with the charge Kondo effect.

Acknowledgments

We are grateful to H. Mukuda for stimulating discussions on the experimental results of ^{125}Te NMR in $\text{Pb}_{1-x}\text{Tl}_x\text{Te}$ ($x=0.01$) prior to publication and urging us to develop the present theory. This

work is supported by the Grant-in-Aid for Scientific Research (Nos. 15K17694 and 17K05555) from the Japan Society for the Promotion of Science.

Appendix A: Equivalence of Pair-Hopping and Inter-orbital Interactions to Pseudo-Spin Exchange Interactions

Here we discuss why the pair-hopping interaction U_{ph} is enhanced in the scattering channel $i\varepsilon_n \rightarrow -i\varepsilon_n$, shown in Figs. A·1 and D·1. The reason why it is enhanced by the charge Kondo effect is understood intuitively by the fact that the pair-hopping interaction is mapped to that of spin-flipping interaction, i.e., the heart of the Kondo interaction, by the canonical transformation for both the localized electron d and conduction electrons with \downarrow spin and \uparrow spin as

$$d_{\downarrow}^{\dagger} \rightarrow \tilde{d}_{\downarrow} \quad \text{and} \quad c_{\mathbf{k}\downarrow}^{\dagger} \rightarrow \tilde{c}_{\mathbf{k}\downarrow}, \quad (\text{A}\cdot 1)$$

$$d_{\uparrow}^{\dagger} \rightarrow \tilde{d}_{\uparrow}^{\dagger} \quad \text{and} \quad c_{\mathbf{k}\uparrow}^{\dagger} \rightarrow \tilde{c}_{\mathbf{k}\uparrow}^{\dagger}. \quad (\text{A}\cdot 2)$$

This is a variant of the canonical transformation introduced by Shiba.^{21,22} Namely, by the transformations [Eqs. (A·1) and (A·2)], the pair-hopping interaction is mapped as follows:

$$\begin{aligned} U_{\text{ph}} \sum_{\mathbf{k}, \mathbf{k}'} \left(d_{\uparrow}^{\dagger} d_{\downarrow}^{\dagger} c_{\mathbf{k}\downarrow} c_{\mathbf{k}'\uparrow} + \text{h.c.} \right) \\ \rightarrow U_{\text{ph}} \sum_{\mathbf{k}, \mathbf{k}'} \left(\tilde{d}_{\uparrow}^{\dagger} \tilde{d}_{\downarrow} \tilde{c}_{\mathbf{k}\downarrow}^{\dagger} \tilde{c}_{\mathbf{k}'\uparrow} + \text{h.c.} \right) \equiv U_{\text{ph}} \left(\tilde{S}_{\text{d}}^{+} \tilde{S}_{\mathbf{k}, \mathbf{k}'}^{-} + \text{h.c.} \right). \end{aligned} \quad (\text{A}\cdot 3)$$

Therefore, the pair-hopping interaction U_{ph} , which is equivalent to $J_{\perp}/2$ in the anisotropic s-d model¹⁸) is enhanced by the Kondo effect in the mapped world. The spin-flipping exchange interaction U_{ph} in the mapped world is represented by the Feynman diagram shown in Fig. A·1(a), while the pair-hopping interaction U_{ph} in the original world is given by the Feynman diagram shown in Fig. A·1(b). Note that the Matsubara frequency of the conduction electrons with \downarrow spin has the opposite sign of that of the \uparrow spin because the direction of propagation in the imaginary time is opposite. Namely, the elastic scattering with $i\varepsilon_n \rightarrow i\varepsilon_n$ in the mapped world causing the Kondo effect corresponds to the scattering with $i\varepsilon_n \rightarrow -i\varepsilon_n$ in the original world. This is the reason why the process shown in Fig. 1 is selectively enhanced.

By the transformation [Eqs. (A·1) and (A·2)], the spin dependent density of states (DOS), $D_{\sigma}(\varepsilon)$, of conduction electrons and localized d electron change from that shown in Fig. A·2(a) to that in Fig. A·2(b). Namely, symmetry with respect to \uparrow and \downarrow spins is broken. Nevertheless, the Kondo effect is possible if the finite DOS of conduction electrons remain at the Fermi level and the energy level of localized electron with \uparrow and \downarrow spins are degenerate, i.e., $\varepsilon_{\text{d}} = -\varepsilon_{\text{d}} - U_{\text{dc}}$, as shown in Fig. A·2. The latter condition is satisfied in the negative- U Anderson model for rather wide doping rates of negative- U ions as discussed in ref. 4. It was also shown by the present authors⁵⁾ that the negative- U effect is realized in the model described by the Hamiltonian [Eq. (1)]. In this sense, it is assured that the condition for zero magnetic field on the localized electron is satisfied in a self-consistent fashion.

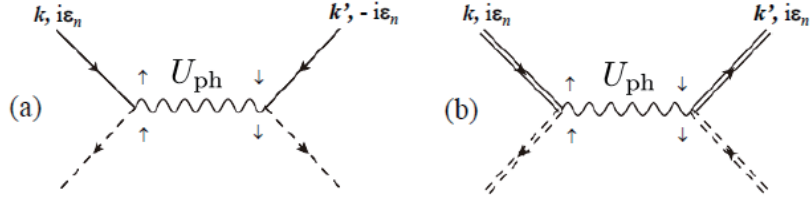


Fig. A-1. (a) Feynman diagram representing the pair-hopping process in the original world, and (b) Feynman diagram representing the spin-flipping exchange process in the mapped world by the canonical transformation [Eqs. (A-1) and (A-2)]. Wavy line represents the pair-hopping interaction U_{ph} , lines with arrow represent the Green function of conduction electrons in the original world, and double lines represent that in the mapped world. Dashed lines with arrow denote the Green functions of the localized electron d both in original and mapped worlds.

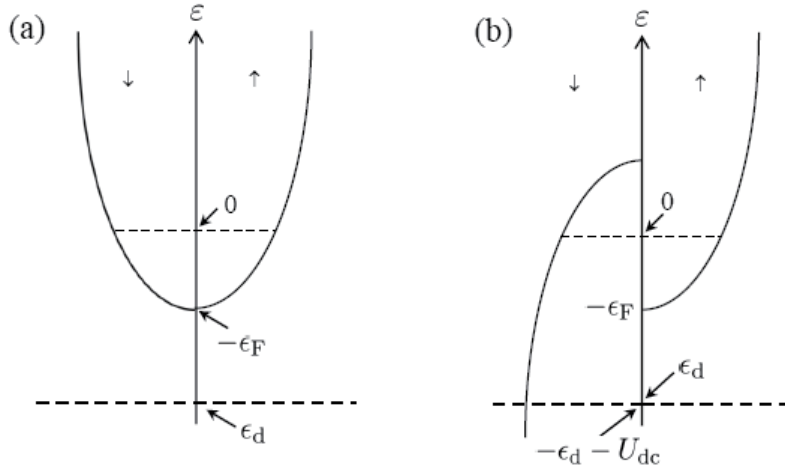


Fig. A-2. Spin dependent DOS, $D_{\sigma}(\varepsilon)$: (a) in the original world, and (b) in the transformed world by the transformation Eqs. (A-1) and (A-2). Note that the origin of energy is ε_F , or energy is measured from ε_F .

Similarly, the inter-orbital interaction U_{dc} is also enhanced by the charge Kondo effect. Indeed, the inter-orbital interaction is mapped by the transformations [Eqs. (A-1) and (A-2)] as follows:

$$\begin{aligned}
 U_{\text{dc}} \sum_{\mathbf{k}, \mathbf{k}'} \sum_{\sigma, \sigma'} d_{\sigma}^{\dagger} d_{\sigma} c_{\mathbf{k}\sigma'} c_{\mathbf{k}'\sigma'} \\
 \rightarrow U_{\text{dc}} \sum_{\mathbf{k}, \mathbf{k}'} (\tilde{d}_{\uparrow}^{\dagger} \tilde{d}_{\uparrow} - \tilde{d}_{\downarrow}^{\dagger} \tilde{d}_{\downarrow}) (\tilde{c}_{\mathbf{k}\uparrow}^{\dagger} \tilde{c}_{\mathbf{k}'\uparrow} - \tilde{c}_{\mathbf{k}\downarrow}^{\dagger} \tilde{c}_{\mathbf{k}'\downarrow}) \equiv 4U_{\text{dc}} \tilde{S}_{\mathbf{k}, \mathbf{k}'}^z \tilde{S}_{\mathbf{k}, \mathbf{k}'}^z.
 \end{aligned} \quad (\text{A}\cdot 4)$$

Therefore, the inter-orbital interaction U_{dc} is enhanced by the Kondo effect in the mapped world because it corresponds to $J_z/4$ in the anisotropic s-d model.⁶⁾ In this sense, the pair-hopping interaction U_{ph} and inter-orbital interaction U_{dc} should be treated impartially as in the case of magnetic Kondo

effect.⁶⁾

Appendix B: Spectral Function of Conduction Electrons

In this Appendix, we derive the spectral function, Eq. (11), for the conduction electrons. First, we note that the Green function $G_c(\mathbf{r}, i\varepsilon_n)$ of conduction electrons with impurity scattering is given by

$$G_c(\mathbf{r}, i\varepsilon_n) = e^{-(r/2\ell)} G_c^{(0)}(\mathbf{r}, i\varepsilon_n), \quad (\text{B}\cdot 1)$$

where ℓ is the mean-free path of the impurity scattering, and $G_c^{(0)}(\mathbf{r}, i\varepsilon_n)$ is the Green function in the pure system without impurity scattering.²³⁾ An explicit form of $G_c^{(0)}(\mathbf{r}, i\varepsilon_n)$ is calculated as follows:

$$\begin{aligned} G_c^{(0)}(\mathbf{r}, i\varepsilon_n) &= \int \frac{d\mathbf{k}}{(2\pi)^3} \frac{e^{i\mathbf{k}\cdot\mathbf{r}}}{i\varepsilon_n - \xi_k} \\ &= \frac{1}{2\pi^2} \frac{1}{r} \int_0^{k_c} dk k \sin(kr) \frac{1}{i\varepsilon_n - \xi_k}, \end{aligned} \quad (\text{B}\cdot 2)$$

where $\xi_k \equiv (k^2/2m) - \mu$, and we have introduced the upper cut-off wave number k_c . Then, the imaginary part of the retarded function $\text{Im}G_c^{(0)\text{R}}(\mathbf{r}, \varepsilon + i\delta)$ is calculated as follows:

$$\begin{aligned} \text{Im}G_c^{(0)\text{R}}(\mathbf{r}, \varepsilon + i\delta) &= -\frac{1}{2\pi} \frac{1}{r} \int_0^{k_c} dk k \sin(kr) \delta(\varepsilon - \xi_k) \\ &= -\frac{m}{2\pi} \frac{1}{r} \int_{-\varepsilon_F}^{\varepsilon_c} d\xi \sin \left[\sqrt{\frac{2m\xi}{k_F^2} + 1} (k_F r) \right] \delta(\varepsilon - \xi) \\ &= -\frac{m}{2\pi} \frac{1}{r} \sin \left[\sqrt{\frac{\varepsilon}{\varepsilon_F} + 1} (k_F r) \right] \theta(\varepsilon + \varepsilon_F) \theta(\varepsilon - \varepsilon_c), \end{aligned} \quad (\text{B}\cdot 3)$$

where we have approximated μ by $-\varepsilon_F$ because we are interested in the low temperature region $T \ll \varepsilon_F$ and ε_c is the upper cut-off energy corresponding to k_c . Therefore, the spectral function $\rho(\mathbf{r}, \varepsilon) \equiv -(1/\pi) \text{Im}G_c^{(0)\text{R}}(\mathbf{r}, \varepsilon + i\delta)$ is given by Eq. (11).

Appendix C: Calculation of $\Gamma_{\text{ph}}^{\text{R}}(\omega + i\delta)$

In this Appendix, we calculate the expression [Eq. (8)] and derive the expression of $\text{Im}\Gamma_{\text{ph}}^{\text{R}}$ [Eq. (14)]. As is justified in Appendix, $G_d(-i\varepsilon_n + i\omega_\nu)G_d(i\varepsilon_n)$ in Eq. (8) can be approximated by $1/\varepsilon_d^2$. Then, $\tilde{\Gamma}_{\text{ph}}(i\omega_\nu) \equiv \Gamma_{\text{ph}}(i\omega_\nu)/T$ [see Eq. (8)] is given as

$$\tilde{\Gamma}_{\text{ph}}(i\omega_\nu) = \frac{2V_{\text{dc}}^2 U_{\text{ph}}}{\varepsilon_d^2} T \sum_{\varepsilon_n} \left(\prod_{\ell=1}^4 \int_{-\infty}^{\infty} dy_\ell \right) \frac{\rho(\mathbf{r}_{ij}, y_1)}{i\varepsilon_n - y_1} \frac{\rho(\mathbf{r}_{ij}, y_2)}{i\varepsilon_n + i\omega_\nu - y_2} \frac{\rho(\mathbf{r}_{ij}, y_3)}{-i\varepsilon_n - y_3} \frac{\rho(\mathbf{r}_{ij}, y_4)}{-i\varepsilon_n + i\omega_\nu - y_4}. \quad (\text{C}\cdot 1)$$

The summation with respect to ε_n is performed in a standard way by transforming the summation to the integration along the axes $\text{Im}z = 0$ and $\text{Im}z = \pm\omega_\nu$ on z -plane, where one is just above these axes and another is just below in the counter direction. The result along $\text{Im}z = 0$, $\Gamma_1(i\omega_\nu)$, is given by

$$\Gamma_1(i\omega_\nu) = \frac{2V_{\text{dc}}^2 U_{\text{ph}}}{\varepsilon_d^2} \left(\prod_{\ell=1}^4 \int_{-\infty}^{\infty} dy_\ell \right) \rho(\mathbf{r}_{ij}, y_1) \rho(\mathbf{r}_{ij}, y_2) \rho(\mathbf{r}_{ij}, y_3) \rho(\mathbf{r}_{ij}, y_4)$$

$$\times \text{th}\left(\frac{y_1}{2T}\right) \frac{1}{y_1 + y_3} \frac{1}{y_1 - y_2 + i\omega_\nu} \frac{1}{-y_1 - y_4 + i\omega_\nu}, \quad (\text{C-2})$$

and those along $\text{Im}z = \pm\omega_\nu$, $\Gamma_{\text{II}}(i\omega_\nu)$, are both given by

$$\Gamma_{\text{II}}(i\omega_\nu) = -\frac{V_{\text{dc}}^2 U_{\text{ph}}}{\epsilon_{\text{d}}^2} \left(\prod_{\ell=1}^4 \int_{-\infty}^{\infty} dy_\ell \right) \rho(\mathbf{r}_{ij}, y_1) \rho(\mathbf{r}_{ij}, y_2) \rho(\mathbf{r}_{ij}, y_3) \rho(\mathbf{r}_{ij}, y_4) \\ \times \text{th}\left(\frac{y_2}{2T}\right) \frac{1}{y_2 - y_1 - i\omega_\nu} \frac{1}{-y_2 - y_3 + i\omega_\nu} \frac{1}{-y_2 - y_4 + 2i\omega_\nu}. \quad (\text{C-3})$$

After analytic continuation, $i\omega_\nu \rightarrow \omega + i\delta$ in Eq. (C-2), and taking an imaginary part, we obtain

$$\text{Im}\Gamma_{\text{I}}^{\text{R}}(\omega + i\delta) = \frac{2\pi V_{\text{dc}}^2 U_{\text{ph}}}{\epsilon_{\text{d}}^2} \left(\prod_{\ell=1}^4 \int_{-\infty}^{\infty} dy_\ell \right) \rho(\mathbf{r}_{ij}, y_1) \rho(\mathbf{r}_{ij}, y_2) \rho(\mathbf{r}_{ij}, y_3) \rho(\mathbf{r}_{ij}, y_4) \\ \times \text{th}\left(\frac{y_4 - \omega}{2T}\right) \frac{1}{y_2 + y_4 - 2\omega} \left[\frac{\delta(y_1 + y_4 - \omega)}{-y_3 + y_4 - \omega} + \frac{\delta(y_1 - y_4 + \omega)}{y_3 + y_4 - \omega} \right], \quad (\text{C-4})$$

where and hereafter the integration implies the principal value integration. In deriving E. (C-4), we have used the property that $\rho(\mathbf{r}_{ij}, y_2)\rho(\mathbf{r}_{ij}, y_4)$ is symmetric with respect to interchange $y_2 \rightleftharpoons y_4$. Similarly, for Eq. (C-3), we obtain

$$\text{Im}\Gamma_{\text{II}}^{\text{R}}(\omega + i\delta) = -\frac{\pi V_{\text{dc}}^2 U_{\text{ph}}}{\epsilon_{\text{d}}^2} \left(\prod_{\ell=1}^4 \int_{-\infty}^{\infty} dy_\ell \right) \rho(\mathbf{r}_{ij}, y_1) \rho(\mathbf{r}_{ij}, y_2) \rho(\mathbf{r}_{ij}, y_3) \rho(\mathbf{r}_{ij}, y_4) \\ \times \text{th}\left(\frac{y_2}{2T}\right) \left\{ \frac{1}{y_2 + y_4 - 2\omega} \left[\frac{\delta(y_2 - y_1 - \omega)}{y_2 + y_3 - \omega} - \frac{\delta(y_2 + y_3 - \omega)}{y_1 - y_2 + \omega} \right] \right. \\ \left. - \frac{\delta(y_2 + y_4 - 2\omega)}{(y_1 - y_2 + \omega)(y_2 + y_3 - \omega)} \right\}. \quad (\text{C-5})$$

Performing the integration with respect to y_1 , Eq. (C-4) is reduced to

$$\text{Im}\Gamma_{\text{I}}^{\text{R}}(\omega + i\delta) = \frac{2\pi V_{\text{dc}}^2 U_{\text{ph}}}{\epsilon_{\text{d}}^2} \left(\prod_{\ell=2}^4 \int_{-\infty}^{\infty} dy_\ell \right) \text{th}\left(\frac{y_4 - \omega}{2T}\right) \frac{\rho(\mathbf{r}_{ij}, y_2) \rho(\mathbf{r}_{ij}, y_3) \rho(\mathbf{r}_{ij}, y_4)}{y_2 + y_4 - 2\omega} \\ \times \left[\frac{\rho(\mathbf{r}_{ij}, y_4 - \omega)}{y_3 + y_4 - \omega} - \frac{\rho(\mathbf{r}_{ij}, \omega - y_4)}{y_3 - y_4 + \omega} \right]. \quad (\text{C-6})$$

Similarly, after performing the integration with respect to y_2 , Eq. (C-5) is reduced to

$$\text{Im}\Gamma_{\text{II}}^{\text{R}}(\omega + i\delta) = -\frac{\pi V_{\text{dc}}^2 U_{\text{ph}}}{\epsilon_{\text{d}}^2} \left(\prod_{\ell=1,3,4} \int_{-\infty}^{\infty} dy_\ell \right) \rho(\mathbf{r}_{ij}, y_1) \rho(\mathbf{r}_{ij}, y_3) \rho(\mathbf{r}_{ij}, y_4) \\ \times \left[\text{th}\left(\frac{y_1}{2T}\right) \frac{\rho(\mathbf{r}_{ij}, y_1 + \omega)}{(-y_1 - y_3)(-y_1 - y_4 + \omega)} - \text{th}\left(\frac{y_3}{2T}\right) \frac{\rho(\mathbf{r}_{ij}, y_3)}{(-y_1 - y_3)(y_3 - y_4 + \omega)} \right. \\ \left. - \text{th}\left(\frac{-y_4 + 2\omega}{2T}\right) \frac{\rho(\mathbf{r}_{ij}, -y_4 + 2\omega)}{(-y_1 - y_4 + \omega)(-y_3 + y_4 - \omega)} \right]. \quad (\text{C-7})$$

By changing the integration variable from y_4 to $y_4 - \omega$, $\text{Im}\Gamma_{\text{I}}^{\text{R}}(\omega + i\delta)$ [E (C-6)] is simplified as

$$\text{Im}\Gamma_{\text{I}}^{\text{R}}(\omega + i\delta) = \frac{2\pi V_{\text{dc}}^2 U_{\text{ph}}}{\epsilon_{\text{d}}^2} \left(\prod_{\ell=2}^4 \int_{-\infty}^{\infty} dy_\ell \right) \text{th}\left(\frac{y_4}{2T}\right) \frac{\rho(\mathbf{r}_{ij}, y_2) \rho(\mathbf{r}_{ij}, y_3) \rho(\mathbf{r}_{ij}, y_4 + \omega)}{y_2 + y_4 - \omega}$$

$$\times \left[\frac{\rho(\mathbf{r}_{ij}, y_4)}{y_3 + y_4} - \frac{\rho(\mathbf{r}_{ij}, -y_4)}{y_3 - y_4} \right]. \quad (\text{C}\cdot 8)$$

Similarly, by changing the integration variables from $y_1 + \omega$ to y_1 in the first term, and from $-y_3 + \omega$ to y_3 and interchanging $y_1 \rightleftharpoons y_3$ in the second term of Eq. (C-7), $\text{Im}\Gamma_{\text{II}}^{\text{R}}(\omega + i\delta)$ [E (C-7)] is simplified as

$$\begin{aligned} \text{Im}\Gamma_{\text{II}}^{\text{R}}(\omega + i\delta) = & -\frac{\pi V_{\text{dc}}^2 U_{\text{ph}}}{\epsilon_{\text{d}}^2} \left(\prod_{\ell=1,3,4} \int_{-\infty}^{\infty} dy_{\ell} \right) \left\{ \text{th} \left(\frac{y_1}{2T} \right) \left[\frac{\rho(\mathbf{r}_{ij}, y_1 - \omega) \rho(\mathbf{r}_{ij}, y_1) \rho(\mathbf{r}_{ij}, y_3) \rho(\mathbf{r}_{ij}, y_4)}{(-y_1 - y_3 + \omega)(-y_1 - y_4 + 2\omega)} \right. \right. \\ & \left. \left. + \frac{\rho(\mathbf{r}_{ij}, y_1 + \omega) \rho(\mathbf{r}_{ij}, -y_1) \rho(\mathbf{r}_{ij}, y_3) \rho(\mathbf{r}_{ij}, y_4)}{(-y_1 - y_3 - \omega)(y_1 - y_4 + 2\omega)} \right] \right. \\ & \left. - \text{th} \left(\frac{-y_4 + \omega}{2T} \right) \frac{\rho(\mathbf{r}_{ij}, y_1) \rho(\mathbf{r}_{ij}, y_3) \rho(\mathbf{r}_{ij}, y_4 + \omega) \rho(\mathbf{r}_{ij}, -y_4 + \omega)}{(y_1 + y_4)(y_3 - y_4)} \right\}. \quad (\text{C}\cdot 9) \end{aligned}$$

To perform the integration with respect to y_2 and y_3 in the first term in the brace of Eq. (C-8), we use the spectral representation, Eq. (10), for the Green function G_{c} . Namely, the real part of the retarded Green function of conduction electrons, $G_{\text{c}}^{\text{R}}(\mathbf{r}, \varepsilon)$, is given by

$$G_{\text{c}}^{\text{R}}(\mathbf{r}, \varepsilon) = \int_{-\infty}^{\infty} dy \frac{\rho(\mathbf{r}, y)}{\varepsilon - y}. \quad (\text{C}\cdot 10)$$

With the use of this relation, Eq. (C-8) is transformed to more compact form as

$$\begin{aligned} \text{Im}\Gamma_{\text{I}}^{\text{R}}(\omega + i\delta) = & \frac{2\pi V_{\text{dc}}^2 U_{\text{ph}}}{\epsilon_{\text{d}}^2} \int_{-\infty}^{\infty} dy_4 \text{th} \left(\frac{y_4}{2T} \right) \rho(\mathbf{r}_{ij}, y_4 + \omega) G_{\text{c}}^{\text{R}}(\mathbf{r}_{ij}, -y_4 + \omega) \\ & \times \left[\rho(\mathbf{r}_{ij}, y_4) G_{\text{c}}^{\text{R}}(\mathbf{r}_{ij}, -y_4) - \rho(\mathbf{r}_{ij}, -y_4) G_{\text{c}}^{\text{R}}(\mathbf{r}_{ij}, y_4) \right]. \quad (\text{C}\cdot 11) \end{aligned}$$

Similarly, Eq. (C-9) is transformed to the following from

$$\begin{aligned} \text{Im}\Gamma_{\text{II}}^{\text{R}}(\omega + i\delta) = & -\frac{\pi V_{\text{dc}}^2 U_{\text{ph}}}{\epsilon_{\text{d}}^2} \left\{ \int_{-\infty}^{\infty} dy_1 \text{th} \left(\frac{y_1}{2T} \right) \right. \\ & \left[\rho(\mathbf{r}_{ij}, y_1 - \omega) \rho(\mathbf{r}_{ij}, y_1) G_{\text{c}}^{\text{R}}(\mathbf{r}_{ij}, -y_1 + \omega) G_{\text{c}}^{\text{R}}(\mathbf{r}_{ij}, -y_1 + 2\omega) \right. \\ & \left. \left. + \rho(\mathbf{r}_{ij}, y_1 + \omega) \rho(\mathbf{r}_{ij}, -y_1) G_{\text{c}}^{\text{R}}(\mathbf{r}_{ij}, -y_1 - \omega) G_{\text{c}}^{\text{R}}(\mathbf{r}_{ij}, y_1 + 2\omega) \right] \right. \\ & \left. + \int_{-\infty}^{\infty} dy_1 \text{th} \left(\frac{y_4 - \omega}{2T} \right) \left[\rho(\mathbf{r}_{ij}, y_4 + \omega) \rho(\mathbf{r}_{ij}, -y_4 + \omega) G_{\text{c}}^{\text{R}}(\mathbf{r}_{ij}, -y_4) G_{\text{c}}^{\text{R}}(\mathbf{r}_{ij}, y_4) \right] \right\}. \quad (\text{C}\cdot 12) \end{aligned}$$

Changing the integration variables from y_1 to $y_1 - \omega$ and from y_1 to $-y_1 + \omega$ in the first and second term in the bracket of Eq. (C-12), the first term in the brace of Eq. (C-12) is transformed to

$$\begin{aligned} -\frac{\pi V_{\text{dc}}^2 U_{\text{ph}}}{\epsilon_{\text{d}}^2} \int_{-\infty}^{\infty} dy_1 \text{th} \left(\frac{y_1 + \omega}{2T} \right) \left[\rho(\mathbf{r}_{ij}, y_1) G_{\text{c}}^{\text{R}}(\mathbf{r}_{ij}, -y_1 + \omega) \rho(\mathbf{r}_{ij}, y_1 + \omega) G_{\text{c}}^{\text{R}}(\mathbf{r}_{ij}, -y_1) \right. \\ \left. - \rho(\mathbf{r}_{ij}, -y_1) G_{\text{c}}^{\text{R}}(\mathbf{r}_{ij}, -y_1 + \omega) \rho(\mathbf{r}_{ij}, y_1 + \omega) G_{\text{c}}^{\text{R}}(\mathbf{r}_{ij}, y_1) \right]. \quad (\text{C}\cdot 13) \end{aligned}$$

By changing the integration variable from y_4 to y_1 in Eq. (C-11), $\text{Im}\Gamma_{\text{I}}^{\text{R}}(\omega + i\delta)$ is transformed to

$$\text{Im}\Gamma_{\text{I}}^{\text{R}}(\omega + i\delta) = \frac{2\pi V_{\text{dc}}^2 U_{\text{ph}}}{\epsilon_{\text{d}}^2} \int_{-\infty}^{\infty} dy_1 \text{th} \left(\frac{y_1}{2T} \right) \rho(\mathbf{r}_{ij}, y_1 + \omega) G_{\text{c}}^{\text{R}}(\mathbf{r}_{ij}, -y_1 + \omega)$$

$$\times \left[\rho(\mathbf{r}_{ij}, y_1) G_c^{\text{R}}(\mathbf{r}_{ij}, -y_1) - \rho(\mathbf{r}_{ij}, -y_1) G_c^{\text{R}}(\mathbf{r}_{ij}, y_1) \right]. \quad (\text{C}\cdot 14)$$

It is easy to see that the expression of integrand in Eq. (C·13) and Eq. (C·14) are same except for the difference of argument x in $\text{th}(x)$. Since the $\text{Im}\Gamma_{\text{II}}(\omega + i\delta)$ arises twice from the integration along $\text{Im}z = \pm\omega_v$, the ω -linear term in twice of Eq. (C·13) and that in Eq. (C·14) cancels with each other in the low temperature region, $T \ll \epsilon_F$, where $\{\text{th}[(y_1 + \omega)/2T] - \text{th}(y_1/2T)\} \approx 2\omega\delta(y_1)$ so that the expression in the bracket in Eq. (C·14) technically vanishes. Therefore, $2\text{Im}\Gamma_{\text{II}}(\omega + i\delta) + \text{Im}\Gamma_{\text{I}}(\omega + i\delta)$ is given by twice of the second term in the brace of Eq. (C·12). Namely, $\text{Im}\tilde{\Gamma}_{\text{ph}}^{\text{R}}(\omega + i\delta) \equiv 2\text{Im}\Gamma_{\text{II}}^{\text{R}}(\omega + i\delta) + \text{Im}\Gamma_{\text{I}}^{\text{R}}(\omega + i\delta)$ is given by

$$\begin{aligned} \text{Im}\tilde{\Gamma}_{\text{ph}}^{\text{R}}(\omega + i\delta) &= -\frac{2\pi V_{\text{dc}}^2 U_{\text{ph}}}{\epsilon_{\text{d}}^2} \int_{-\infty}^{\infty} dy_4 \text{th}\left(\frac{y_4 - \omega}{2T}\right) \\ &\quad \times \left[\rho(\mathbf{r}_{ij}, y_4 + \omega) \rho(\mathbf{r}_{ij}, -y_4 + \omega) G_c^{\text{R}}(\mathbf{r}_{ij}, -y_4) G_c^{\text{R}}(\mathbf{r}_{ij}, y_4) \right] \\ &= -\frac{2\pi V_{\text{dc}}^2 U_{\text{ph}}}{\epsilon_{\text{d}}^2} \int_{-\infty}^{\infty} dy_4 \left[\text{th}\left(\frac{y_4 - \omega}{2T}\right) - \text{th}\frac{y_4}{2T} \right] \\ &\quad \times \left[\rho(\mathbf{r}_{ij}, y_4 + \omega) \rho(\mathbf{r}_{ij}, -y_4 + \omega) G_c^{\text{R}}(\mathbf{r}_{ij}, -y_4) G_c^{\text{R}}(\mathbf{r}_{ij}, y_4) \right], \quad (\text{C}\cdot 15) \end{aligned}$$

where, in deriving the second equality, we have used the fact that the function in the bracket is an even function in y_4 so that the term including $\text{th}(y_4/2T)$ vanishes.

Appendix D: Case of direct overlap of electrons between Tl and Te sites

In the case where the localized state at Tl site extends to the adjacent Te site, the relaxation function Γ' , corresponding to $\tilde{\Gamma}_{\text{ph}}$ defined by Eq. (C·1), is derived from the Feynman diagram shown in Fig. D·1 and its vertical inversion. Its analytic expression is given by

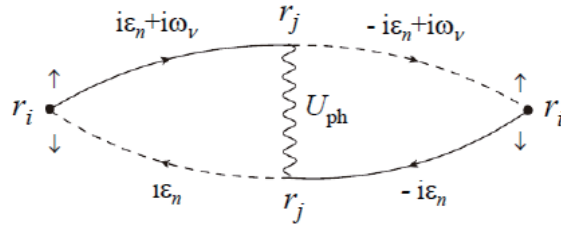


Fig. D·1. Feynman diagram giving the NMR longitudinal relaxation rates $1/T_1T$ at Te (\mathbf{r}_i) site, in the case where 6s electron at Tl (\mathbf{r}_j) site extends to the Te (\mathbf{r}_i) site.

$$\Gamma'(i\omega_v) = 2U_{\text{ph}}T \sum_{\epsilon_n} G_c(\mathbf{r}_{ij}, i\epsilon_n + i\omega_v) G_c(\mathbf{r}_{ij}, -i\epsilon_n)$$

$$\times G_d(-i\varepsilon_n + i\omega_\nu)G_d(i\varepsilon_n) \quad (\text{D}\cdot 1)$$

Instead of Eq. (C-1), we obtain.

$$\Gamma'(i\omega_\nu) = 2U_{\text{ph}}T \sum_{\varepsilon_n} \left(\prod_{\ell=2}^3 \int_{-\infty}^{\infty} dy_\ell \right) \frac{\rho(\mathbf{r}_{ij}, y_2)}{i\varepsilon_n + i\omega_\nu - y_2} \frac{\rho(\mathbf{r}_{ij}, y_3)}{-i\varepsilon_n - y_3} \frac{1}{i\varepsilon_n - \varepsilon_d} \frac{1}{-i\varepsilon_n + i\omega_\nu - \varepsilon_d} \quad (\text{D}\cdot 2)$$

Note that we have not approximated $G_d(-i\varepsilon_n)G_d(-i\varepsilon_n)$ by $1/\varepsilon_d^2$. The summation in Eq. (D-2) with respect to ε_n is performed in a standard way by transforming the summation to the integration along the axes $\text{Im}z = 0$ and $\text{Im}z = \pm\omega_\nu$ on z -plane, where one is just above these axes and another is just below in the counter direction. The result is

$$\begin{aligned} \Gamma'(i\omega_\nu) &= U_{\text{ph}} \left(\prod_{\ell=2}^3 \int_{-\infty}^{\infty} dy_\ell \right) \rho(\mathbf{r}_{ij}, y_2)\rho(\mathbf{r}_{ij}, y_3) \\ &\times \left\{ \frac{1}{y_3 + \varepsilon_d} \left[\text{th}\left(\frac{y_3}{2T}\right) \frac{1}{-y_2 - y_3 + i\omega_\nu} \frac{1}{y_3 - \varepsilon_d + i\omega_\nu} + \text{th}\left(\frac{\varepsilon_d}{2T}\right) \frac{1}{\varepsilon_d - y_2 + i\omega_\nu} \frac{1}{-2\varepsilon_d + i\omega_\nu} \right] \right. \\ &\left. + \frac{1}{y_2 + \varepsilon_d - 2i\omega_\nu} \left[\text{th}\left(\frac{y_2}{2T}\right) \frac{1}{-y_2 - y_3 + i\omega_\nu} \frac{1}{y_2 - \varepsilon_d - i\omega_\nu} + \text{th}\left(\frac{\varepsilon_d}{2T}\right) \frac{1}{\varepsilon_d - y_3 - i\omega_\nu} \frac{1}{-2\varepsilon_d + i\omega_\nu} \right] \right\} \end{aligned}$$

After analytic continuation, $i\omega_\nu \rightarrow \omega + i\delta$ in Eq. (D-3), and taking an imaginary part, we obtain

$$\begin{aligned} \text{Im}\Gamma'^{\text{R}}(\omega + i\delta) &= -\pi U_{\text{ph}} \left(\prod_{\ell=2}^3 \int_{-\infty}^{\infty} dy_\ell \right) \rho(\mathbf{r}_{ij}, y_2)\rho(\mathbf{r}_{ij}, y_3) \frac{1}{y_3 + \varepsilon_d} \\ &\times \left\{ \text{th}\left(\frac{y_3}{2T}\right) \left[\frac{\delta(y_3 - \varepsilon_d + \omega)}{-y_2 - y_3 + \omega} + \frac{\delta(y_2 + y_3 - \omega)}{y_3 - \varepsilon_d + \omega} \right] \right. \\ &\left. + \text{th}\left(\frac{\varepsilon_d}{2T}\right) \left[\frac{\delta(-2\varepsilon_d + \omega)}{\varepsilon_d - y_2 + \omega} + \frac{\delta(\varepsilon_d - y_2 + \omega)}{-2\varepsilon_d + \omega} \right] \right\} \\ &+ \pi U_{\text{ph}} \left(\prod_{\ell=2}^3 \int_{-\infty}^{\infty} dy_\ell \right) \rho(\mathbf{r}_{ij}, y_2)\rho(\mathbf{r}_{ij}, y_3) \\ &\times \left\{ \text{th}\left(\frac{y_2}{2T}\right) \frac{1}{-y_2 - \varepsilon_d + 2\omega} \left[\frac{\delta(y_2 + y_3 - \omega)}{y_2 - \varepsilon_d - \omega} + \frac{\delta(y_2 - \varepsilon_d - \omega)}{y_2 + y_3 - \omega} \right] \right. \\ &\left. - \text{th}\left(\frac{y_2}{2T}\right) \frac{\delta(y_2 + \varepsilon_d - 2\omega)}{(y_2 + y_3 - \omega)(y_2 - \varepsilon_d - \omega)} \right. \\ &\left. + \text{th}\left(\frac{\varepsilon_d}{2T}\right) \frac{1}{-2\varepsilon_d + \omega} \left[\frac{\delta(y_2 + \varepsilon_d - 2\omega)}{\varepsilon_d - y_3 - \omega} + \frac{\delta(y_3 - \varepsilon_d + \omega)}{\varepsilon_d + y_2 - 2\omega} \right] \right\} \quad (\text{D}\cdot 4) \end{aligned}$$

Performing the integration with respect to y_2 or y_3 , Eq. (D-4) is reduced to

$$\begin{aligned} \text{Im}\Gamma'^{\text{R}}(\omega + i\delta) &= -\pi U_{\text{ph}} \int_{-\infty}^{\infty} dy_2 \rho(\mathbf{r}_{ij}, y_2) \\ &\times \left\{ \left[\text{th}\left(\frac{\varepsilon_d - \omega}{2T}\right) - \text{th}\left(\frac{\varepsilon_d}{2T}\right) \right] \frac{\rho(\mathbf{r}_{ij}, \varepsilon_d - \omega)}{(-\varepsilon_d - y_2 + 2\omega)(2\varepsilon_d - \omega)} \right. \\ &\left. + \left[\text{th}\left(\frac{\varepsilon_d - 2\omega}{2T}\right) - \text{th}\left(\frac{\varepsilon_d}{2T}\right) \right] \frac{\rho(\mathbf{r}_{ij}, -\varepsilon_d + 2\omega)}{(-\varepsilon_d + y_2 + \omega)(2\varepsilon_d - \omega)} \right\} \end{aligned}$$

$$\begin{aligned}
& - \left[\text{th} \left(\frac{y_2 - \omega}{2T} \right) - \text{th} \left(\frac{y_2}{2T} \right) \right] \frac{\rho(\mathbf{r}_{ij}, -y_2 + \omega)}{(-y_2 - \epsilon_d + 2\omega)(-y_2 + \epsilon_d + \omega)} \\
& + \left[\text{th} \left(\frac{\epsilon_d}{2T} \right) - \text{th} \left(\frac{\epsilon_d + \omega}{2T} \right) \right] \frac{\rho(\mathbf{r}_{ij}, \epsilon_d + \omega)}{(y_2 + \epsilon_d)(-2\epsilon_d + \omega)}. \tag{D-5}
\end{aligned}$$

The first and fourth terms give only vanishing contribution because $\rho(\mathbf{r}_{ij}, \epsilon_d)$ [Eq. (11)] are vanishing in the present case $\epsilon_d < -\epsilon_F$. The second term also gives vanishing contribution because $\{\text{th}[(\epsilon_d - 2\omega)/2T] - \text{th}(\epsilon_d/2T)\}$ is vanishing if the ϵ_d is located well below the bottom of the conduction band (in the hole picture). Therefore, Eq. (D-5) is finally reduced to

$$\text{Im}\Gamma'^R(\omega + i\delta) = \pi U_{\text{ph}} \int_{-\infty}^{\infty} dy_2 \left[\text{th} \left(\frac{y_2 - \omega}{2T} \right) - \text{th} \frac{y_2}{2T} \right] \frac{\rho(\mathbf{r}_{ij}, y_2)\rho(\mathbf{r}_{ij}, -y_2 + \omega)}{(-y_2 - \epsilon_d + 2\omega)(-y_2 + \epsilon_d + \omega)}. \tag{D-6}$$

Then, up to the linear term in ω , $\text{Im}\Gamma'(\omega + i\delta)$ is given as

$$\text{Im}\Gamma'^R(\omega + i\delta) \approx -\omega \pi U_{\text{ph}} \int_{-\infty}^{\infty} dy_2 \frac{\partial \text{th} \left(\frac{y_2}{2T} \right)}{\partial y_2} \frac{\rho(\mathbf{r}_{ij}, y_2)\rho(\mathbf{r}_{ij}, -y_2)}{(-y_2 - \epsilon_d)(-y_2 + \epsilon_d)}. \tag{D-7}$$

Considering that $\rho(\mathbf{r}_{ij}, y_2)\rho(\mathbf{r}_{ij}, -y_2 + \omega)$ with $\omega \approx 0$ is vanishing at $|y_2| > \epsilon_F$ and $|\epsilon_d| \gg \epsilon_F$, the expression [Eq. (D-7)] is further simplified as

$$\begin{aligned}
\text{Im}\Gamma'^R(\omega + i\delta) & \approx \omega \frac{\pi U_{\text{ph}}}{\epsilon_d^2} \int_{-\infty}^{\infty} dy_2 \frac{\partial \text{th} \left(\frac{y_2}{2T} \right)}{\partial y_2} \rho(\mathbf{r}_{ij}, y_2)\rho(\mathbf{r}_{ij}, -y_2) \\
& \approx \omega \frac{2\pi U_{\text{ph}}}{\epsilon_d^2} [\rho(\mathbf{r}_{ij}, 0)]^2. \tag{D-8}
\end{aligned}$$

If $G_d(i\epsilon_n + i\omega_\nu)G_d(-i\epsilon_n)$ in Eq. (D-1) is approximated by $1/\epsilon_d^2$ as in Eq. (C-1), the relaxation function $\Gamma''(i\omega_\nu)$ is easily calculated as follows:

$$\begin{aligned}
\Gamma''^R(i\omega_\nu) & = \frac{2U_{\text{ph}}}{\epsilon_d^2} T \sum_{\epsilon_n} G_c(\mathbf{r}_{ij}, i\epsilon_n + i\omega_\nu) G_c(\mathbf{r}_{ij}, -i\epsilon_n) \\
& = \frac{2U_{\text{ph}}}{\epsilon_d^2} T \sum_{\epsilon_n} \left(\prod_{\ell=2}^3 \int_{-\infty}^{\infty} dy_\ell \right) \frac{\rho(\mathbf{r}_{ij}, y_2)}{i\epsilon_n + i\omega_\nu - y_2} \frac{\rho(\mathbf{r}_{ij}, y_3)}{-i\epsilon_n - y_3} \\
& = \frac{2U_{\text{ph}}}{\epsilon_d^2} \left(\prod_{\ell=2}^3 \int_{-\infty}^{\infty} dy_\ell \right) \frac{1}{2} \left(\text{th} \frac{y_2}{2T} + \text{th} \frac{y_3}{2T} \right) \frac{\rho(\mathbf{r}_{ij}, y_2)\rho(\mathbf{r}_{ij}, y_3)}{-y_2 - y_3 + i\omega_\nu} \tag{D-9}
\end{aligned}$$

After analytic continuation, $i\omega_\nu \rightarrow \omega + i\delta$ in Eq. (D-9), and performing an integration with respect to y_3 , $\text{Im}\Gamma''^R(\omega + i\delta)$ is reduced to

$$\text{Im}\Gamma''^R(\omega + i\delta) = \frac{2\pi U_{\text{ph}}}{\epsilon_d^2} \int_{-\infty}^{\infty} dy_2 \frac{1}{2} \left[\text{th} \frac{y_2}{2T} - \text{th} \left(\frac{y_2 - \omega}{2T} \right) \right] \rho(\mathbf{r}_{ij}, y_2)\rho(\mathbf{r}_{ij}, -y_2 + \omega). \tag{D-10}$$

Then, up to the linear order in ω , $\text{Im}\Gamma''(\omega + i\delta)$ is given as

$$\begin{aligned}
\text{Im}\Gamma''^R(\omega + i\delta) & \approx \omega \frac{\pi U_{\text{ph}}}{\epsilon_d^2} \int_{-\infty}^{\infty} dy_2 \frac{\partial \text{th} \left(\frac{y_2}{2T} \right)}{\partial y_2} \rho(\mathbf{r}_{ij}, y_2)\rho(\mathbf{r}_{ij}, -y_2) \\
& \approx \omega \frac{2\pi U_{\text{ph}}}{\epsilon_d^2} [\rho(\mathbf{r}_{ij}, 0)]^2, \tag{D-11}
\end{aligned}$$

which is the same as the expression [Eq. (D·8)]. This justifies the approximation $G_d(i\varepsilon_n + i\omega_\nu)G_d(-i\varepsilon_n) \approx 1/\epsilon_d^2$ in Eq. (D·1), which in turn justifies the same approximation adopted in Eq. (C·1). A physical basis of this justification is that the $\text{Im}\Gamma^R(\omega + i\delta)$ arises only from the low energy processes associated with conduction electrons described by $G_c(\mathbf{r}_{ij}, i\varepsilon_n + i\omega_\nu)$ and $G_c(\mathbf{r}_{ij}, -i\varepsilon_n)$ in Eq. (D·1), so that the same approximation is expected to remain valid also in the calculation of $\text{Im}\tilde{\Gamma}_{\text{ph}}^R(\omega + i\delta)$ performed in Appendix .

In the limit $k_F|\mathbf{r}_{ij}| \ll 1$, with the use of asymptotic form of $\rho(\mathbf{r}, y)$ [Eq. (12)], Eq. (D·11) is estimated as

$$\text{Im}\Gamma^R(\omega + i\delta) \approx \omega \frac{2\pi N_F^2}{\epsilon_d^2} e^{-(|\mathbf{r}_{ij}|/\ell)} U_{\text{ph}} + O(\omega^2). \quad (\text{D}\cdot 12)$$

Then, the NMR relaxation rate $1/T_1 T$ is given by

$$\frac{1}{T_1 T} = A^2 \frac{2\pi N_F^2}{\epsilon_d^2} e^{-(|\mathbf{r}_{ij}|/\ell)} U_{\text{ph}}. \quad (\text{D}\cdot 13)$$

Appendix E: Real-Part of Retarded Green Function of Conduction Electrons

In this Appendix, we derive an analytic form of $G_c^R(\mathbf{r}, \varepsilon)$ [Eq. (17)] in the limit $k_F r \ll 1$, where $G_c^R(\mathbf{r}, \varepsilon)$ is approximated by

$$G_c^R(\mathbf{r}, \varepsilon) \approx -\frac{mk_F}{2\pi^2} e^{-(r/2\ell)} \frac{1}{\sqrt{\epsilon_F}} \int_{-\epsilon_F}^{\epsilon_c} dy \frac{\sqrt{y + \epsilon_F}}{y - \varepsilon}. \quad (\text{E}\cdot 1)$$

Integration with respect to y is performed by elementary integral leading to the following results. In the case $\varepsilon + \epsilon_F > 0$,

$$\int_{-\epsilon_F}^{\epsilon_c} dy \frac{\sqrt{y + \epsilon_F}}{y - \varepsilon} = 2\sqrt{\epsilon_c + \epsilon_F} + \sqrt{\varepsilon + \epsilon_F} \log \left| \frac{\sqrt{\epsilon_c + \epsilon_F} - \sqrt{\varepsilon + \epsilon_F}}{\sqrt{\epsilon_c + \epsilon_F} + \sqrt{\varepsilon + \epsilon_F}} \right|, \quad (\text{E}\cdot 2)$$

while in the case $\varepsilon + \epsilon_F < 0$,

$$\int_{-\epsilon_F}^{\epsilon_c} dy \frac{\sqrt{y + \epsilon_F}}{y - \varepsilon} = 2\sqrt{\epsilon_c + \epsilon_F} - 2\sqrt{-\varepsilon - \epsilon_F} \tan^{-1} \frac{\sqrt{\epsilon_c + \epsilon_F}}{\sqrt{-\varepsilon - \epsilon_F}}. \quad (\text{E}\cdot 3)$$

Appendix F: Calculation of $J(k_F r)$ in the limit $k_F r \gg 1$

In this Appendix, we derive an asymptotic form of $J(k_F r)$, Eq. (19), in the limit $k_F r \gg 1$. The integration in Eq. (19) with respect to y , which is denoted by K , is transformed, by changing the integration variable from y to $u \equiv \sqrt{(y/\epsilon_F) + 1}$ and defining $\Lambda \equiv \sqrt{(\epsilon_c/\epsilon_F) + 1}$, as follows:

$$\begin{aligned} K &= \int_0^\Lambda du \frac{2u}{(u+1)(u-1)} \sin[(k_F r)u] \\ &= \text{Im} \left[\int_0^\Lambda du \frac{2u}{(u+1)(u-1)} e^{i(k_F r)u} \right], \end{aligned} \quad (\text{F}\cdot 1)$$

where the integration with respect to u is the principal integration for avoiding the singularity around $u = 1$.

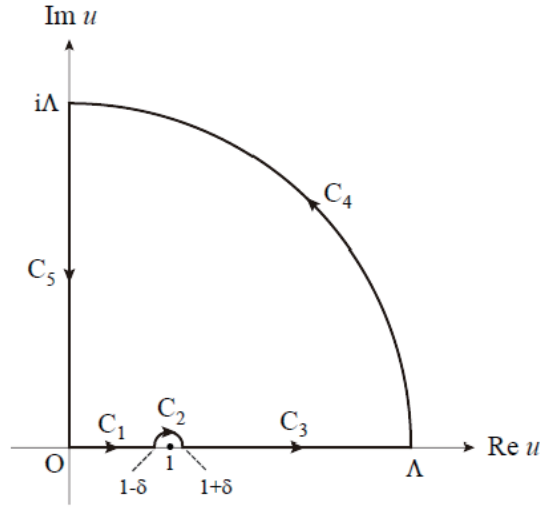


Fig. F.1. Path of contour integration in Eq. (F.1) in the complex- u plane.

Let us define K_i ($i = 1 \sim 5$) by integration with respect complex u along the path C_i shown in Fig. F.1 as

$$K_i \equiv \int_{C_i} du \frac{2u}{(u+1)(u-1)} e^{i(k_{Fr})u}. \quad (F.2)$$

An infinitesimally small positive number δ in Fig. F.1 will be tended to zero after calculations. $\lim_{\delta \rightarrow 0} [K_1(\delta) + K_3(\delta)]$ is the same as the principal integration in Eq. (F.1). The integration along C_2 , a semicircle with the radius δ , is performed in the limit $\delta \rightarrow 0$ as

$$\begin{aligned} K_2 &= \int_{\pi}^0 d(\delta e^{i\varphi}) \frac{2(1 + \delta e^{i\varphi})}{(2 + \delta e^{i\varphi}) \delta e^{i\varphi}} e^{i(k_{Fr})(1 + \delta e^{i\varphi})} \\ &\approx i \int_{\pi}^0 d\varphi e^{i(k_{Fr})} = -i \pi \cos(k_{Fr}) + \pi \sin(k_{Fr}). \end{aligned} \quad (F.3)$$

It is easy to see that $K_5(\Lambda)$ is real and finite number. The integration along C_4 , a semicircle with the radius Λ , is performed as

$$\begin{aligned} K_4(\Lambda) &= \int_0^{\pi/2} d(\Lambda e^{i\theta}) \frac{2\Lambda e^{i\theta}}{\Lambda^2 e^{2i\theta} - 1} e^{[i(k_{Fr})\Lambda e^{i\theta}]} \\ &= i \int_0^{\pi/2} d\theta \frac{2\Lambda^2 e^{2i\theta}}{\Lambda^2 e^{2i\theta} - 1} e^{i(k_{Fr})\Lambda \cos \theta} e^{-(k_{Fr})\Lambda \sin \theta}. \end{aligned} \quad (F.4)$$

It is shown by a standard way of calculus that $K_4(\Lambda)$ vanishes in proportion to $1/(k_{Fr})$ in the limit $k_{Fr} \gg 1$.

Therefore, Eq. (F.1) is transformed in the limit $k_{Fr} \gg 1$ as follows:

$$K = \lim_{\delta \rightarrow 0} \text{Im}[K_1(\delta) + K_3(\delta)]$$

$$= \lim_{\delta \rightarrow 0} \text{Im} \left\{ [K_1(\delta) + K_3(\delta) + K_2(\delta) + K_4 + K_5] - [K_2(\delta) + K_4 + K_5] \right\} \quad (\text{F}\cdot\text{5})$$

$$= - \lim_{\delta \rightarrow 0} \text{Im} [K_2(\delta) + K_4 + K_5] \quad (\text{F}\cdot\text{6})$$

$$\approx - \lim_{\delta \rightarrow 0} \text{Im} K_2(\delta) = \pi \cos(k_{\text{F}r}). \quad (\text{F}\cdot\text{7})$$

In deriving Eq. (F·6) from Eq. (F·5), we have used the fact that the contour integration in the complex- u plane along the path shown in Fig. F·1 vanishes because the integrand is an analytic function in the domain encircled by the contour. In deriving Eq. (F·7) from Eq. (F·6), we have used Eq. (F·3).

As a result, $J(k_{\text{F}r})$ [Eq. (19)] in the limit $k_{\text{F}r} \gg 1$ is given by

$$J(k_{\text{F}r}) \approx \frac{1}{k_{\text{F}r}} \pi \cos(k_{\text{F}r}). \quad (\text{F}\cdot\text{8})$$

Appendix G: Poorman's Scaling Analysis for U_{ph} and U_{dc}

In this Appendix, we perform the poorman's scaling analysis for the pair-hopping interaction U_{ph} and the inter-orbital interaction U_{dc} to investigate renormalization effect on these interaction. As discussed in Appendix, in the mapped world, U_{ph} and U_{dc} correspond to $J_{\perp}/2$ and $J_z/4$ in the anisotropic s-d model. The evolution equations for these dimensionless coupling constants, $y_{\perp} \equiv J_{\perp}N_{\text{F}}$ and $y_z \equiv J_zN_{\text{F}}$ are given as follows:¹⁸⁾

$$\frac{dy_{\perp}}{dx} = -y_{\perp}y_z, \quad (\text{G}\cdot\text{1})$$

$$\frac{dy_z}{dx} = -y_{\perp}^2, \quad (\text{G}\cdot\text{2})$$

where $x \equiv \log(E_c/E_c^0)$ with E_c and E_c^0 being the renormalized and bare bandwidths, respectively. It is well known that $y_{\perp}^2 - y_z^2 = \text{const.} \equiv C$. Substituting $y_{\perp}^2 = y_z^2 + C$ into Eq. (G·2), the evolution equation of y_z [Eq. (G·2)] is reduced to

$$\frac{dy_z}{dx} = -(y_z^2 + C). \quad (\text{G}\cdot\text{3})$$

The solution of this differential equation is easily solved: In the case $C \equiv a^2 > 0$,

$$y_z(x) = \frac{y_z^0 - a \tan(ax)}{1 + \frac{y_z^0}{a} \tan(ax)}, \quad (\text{G}\cdot\text{4})$$

where y_z^0 is the initial value of y_z at $x = 0$. Similarly, in the case $C \equiv -b^2 < 0$, the solution is given as

$$y_z(x) = \frac{y_z^0 + b \tanh(bx)}{1 + \frac{y_z^0}{b} \tanh(bx)}. \quad (\text{G}\cdot\text{5})$$

In the high temperature region, $T \gtrsim T_K$, where $|x| \ll 1$, both $y_z(x)$ [Eq. (G-4)] and $y_\perp(x)$ [Eq. (G-5)] are expressed as

$$y_z(x) \approx y_z^0 - (y_\perp^0)^2 x + \dots \quad (\text{G-6})$$

With the use of this approximate expression, that for y_\perp is easily obtained in the following form

$$y_\perp(x) \approx y_\perp^0 - y_\perp^0 y_z^0 x + \dots \quad (\text{G-7})$$

Therefore, in the high temperature region $T \gtrsim T_K$, temperature dependence of $U_{\text{ph}} = (J_\perp/2)$ and $U_{\text{dc}} = (J_z/4)$ are given as follows:

$$U_{\text{ph}}(T) = \frac{1}{2N_F} y_\perp \left(\log \frac{T}{E_c^0} \right) \approx \frac{1}{2} \left[2U_{\text{ph}}^0 - 8N_F U_{\text{ph}} U_{\text{dc}}^0 \log \frac{T}{E_c^0} \right], \quad (\text{G-8})$$

$$U_{\text{dc}}(T) = \frac{1}{4N_F} y_z \left(\log \frac{T}{E_c^0} \right) \approx \frac{1}{4} \left[4U_{\text{dc}}^0 - N_F (2U_{\text{ph}}^0)^2 \log \frac{T}{E_c^0} \right], \quad (\text{G-9})$$

where U_{ph}^0 and U_{dc}^0 are bare couplings. Namely, both $U_{\text{ph}}(T)$ and $U_{\text{dc}}(T)$ exhibit logarithmic increase toward $T = T_K$ at which $y_\perp(x)$ and $y_z(x)$ diverges at the level of approximation of the poorman's scaling.¹⁸⁾

On the other hand, both $y_\perp(E)$ and $y_z(E)$ diverge toward $E = T_K$ as

$$y_\perp(E) = \frac{y_\perp(0)}{1 + y_\perp(0) \log \frac{E}{E_c^0}} = \frac{1}{\log \frac{E}{T_K}} \approx y_z(E), \quad (\text{G-10})$$

where T_K is given by the solution for the case $C = 0$ as $T_K = E_c^0 e^{-y_\perp(0)}$ or $[1 + y_\perp(0) \log(T_K/E_c^0)] = 0$. Of course, this divergence at $E = T_K$ is an artifact due to the one-loop order approximation, but true divergence occurs in the limit $E \ll T_K$. Namely, the expression [Eq.(G-10)] is not valid very near at $E = T_K$ while it gives growing tendency of $y_\perp(E)$ and $y_z(E)$ toward $E = T_K$

References

- 1) Y. Matsushita, H. Bluhm, T. H. Geballe, and I. R. Fisher, *Phys. Rev. Lett.* **94**, 157002 (2005).
- 2) R. D. Shannon, *Acta Cryst. A* **32**, 751 (1976).
- 3) M. Dzero and J. Schmalian, *Phys. Rev. Lett.* **94**, 157003 (2005).
- 4) A. Taraphder and P. Coleman, *Phys. Rev. Lett.* **66**, 2814 (1991).
- 5) H. Matsuura and K. Miyake, *J. Phys. Soc. Jpn.* **81**, 113705 (2012).
- 6) P. W. Anderson, *Phys. Rev. Lett.* **34**, 953 (1975).
- 7) H. Katayama-Yoshida and A. Zunger, *Phys. Rev. Lett.* **55**, 1618 (1985).
- 8) I. Hase and T. Yanagisawa, *Phys. Rev. B* **76**, 174103 (2007).
- 9) W. A. Harrison, *Phys. Rev. B* **74**, 245128 (2006).
- 10) A. C. Hewson and D. Meyer, *J. Phys. Condens. Matter* **14**, 427 (2002).
- 11) T. Hotta, *J. Phys. Soc. Jpn.* **76**, 084702 (2007).
- 12) R. Shinzaki, J. Nasu, and A. Koga, *Phys Rev B* **97**, 125130 (2018).
- 13) H. Mukuda, T. Matsumura, S. Maki, M. Yashima, Y. Kitaoka, H. Murakami, K. Miyake, P. Giraldo-Gallo, T. H. Geballe, and I. R. Fisher, *J. Phys. Soc. Jpn.* **87** 023706 (2018).
- 14) T. Moriya, *J. Phys. Soc. Jpn.* **18**, 516 (1963).
- 15) K. Maki, *Prog. Theor. Phys.* **40**, 193 (1968).
- 16) R. S. Thompson, *Phys. Rev. B* **1**, 327 (1970).
- 17) L. G. Aslamasova and A. I. Larkin, *Phys. Lett. A* **26**, 238 (1968).
- 18) P. W. Anderson, *J. Phys. C* **3**, 2436 (1970).
- 19) See, for example, J. M. Ziman, *Principles of The Theory of Solids* (Cambridge University Press, London, 1972) 2nd ed., Sect. 5.2.
- 20) K. Miyake and S. Watanabe, arXiv:1706.03328.
- 21) H. Shiba: *Prog. Theor. Phys.* **48**, 2171 (1972).
- 22) R. Micnas, J. Ranninger, and S. Robaszkiewicz, *Rev. Mod. Phys.* **62**, 113 (1990).
- 23) A. A. Abrikosov, L. P. Gor'kov, and I. Ye. Dzyaloshinskii, *Quantum Field Theoretical Methods in Statistical Physics* (Pergamon, Oxford, U.K., 1965) 2nd ed., Sect. 39.2.
- 24) K. Yosida, *Phys. Rev.* **147**, 223 (1966); *Prog. Theor. Phys.* **36**, 875 (1966).
- 25) A. Yoshimori and K. Yosida, *Prog. Theor. Phys.* **39**, 1413 (1968).
- 26) P. Nozières, *J. Low Temp. Phys.* **17**, 31 (1974).
- 27) H. Shiba, *Prog. Theor. Phys.* **54**, 967 (1975).
- 28) S. Yotsuhashi, K. Miyake, and H. Kusunose, *Physica B* **312-313**, 100 (2002).
- 29) S. Yotsuhashi, K. Miyake, and H. Kusunose, *J. Phys. Soc Jpn.* **85** (2016) 034719.
- 30) H. Tou, Y. Kitaoka, K. Ishida, K. Asayama, N. Kimura, Y. Ōnuki, E. Yamamoto, H. Haga and K. Maezawa, *Phys. Rev. Lett.* **80**, 3129 (1998); private communications.
- 31) Y. Kohori, T. Kohara, H. Shibai, Y. Oda, Y. Kitaoka, and K. Asayama, *J. Phys. Soc. Jpn.* **57**, 395 (1988).